Evidence for belief updating in decision-variable space: past decisions with finer granularity attract future ones more strongly

Heeseung Lee[1,2,✉], Jaeseob Lim[1], and Sang-Hun Lee[1,✉]

[1]Department of Brain and Cognitive Sciences, Seoul National University, Seoul, Republic of Korea.
[2]Department of Psychological and Brain Sciences, Dartmouth College, Hanover, NH, USA.
✉e-mail: heeseung1990@gmail.com; visionsl@snu.ac.kr

Abstract

Essential to adaptive intelligence is the ability to create mental spaces where knowledge from past experiences cumulates and integrates with newly acquired information. When engaged in decision-making tasks, humans are known to create such a space and therein form decision variables, which integrate task-essential information from multiple sources in a generalizable form. Much effort has focused on the cognitive and neural processes involved in forming decision variables. However, there is limited understanding of how decision variables, once formed, are utilized to adapt to the environment. Considering the abstract and generalizable nature of decision variables, we reason that decision-makers would benefit from shaping and updating probabilistic knowledge—known as *belief*—within the decision-variable space. As one such belief updating, we hypothesize that an act of decision commitment restricts the current belief about the decision variable to a range of states corresponding to that decision. This implies that past decisions not only attract future ones but also exert a greater pull when those decisions are made with finer granularity—dubbed 'the granularity effect.' Here, we present the findings of seven psychophysical experiments that consistently confirm these implications while ruling out the stimulus and action space as potential loci of the granularity effect. Further, as a principled and unified account of the granularity effect and other history effects found in various perceptual tasks, we offer a Bayesian model where beliefs are updated separately in the stimulus and decision-variable spaces. Our work demonstrates how humans leverage the abstract and generalizable nature of the decision-variable space to effectively adapt to their surroundings, expanding the gamut of human intellect.

Introduction

Making sound decisions is crucial for all living beings to survive and thrive, enabling them to take appropriate courses of action in diverse situations they face. All commanding decision theories[1-5], despite their nuanced differences in formalism, point towards the need for constructing general cognitive quantity that can accommodate various sensory-motor mappings[6-8]. Such a need entails creating an internal space for abstract representation, where decision variables (DVs) are encoded through the integration of current evidence, prior knowledge, and learned cost[9,10]. Within this representational space[11], dubbed 'DV space,' various operations are then carried out on DV to guide our course of action[2]. The DV space holds great significance in understanding the abstract nature and general applicability of adaptive intelligence[12]. The encoded state (value) of DV is *abstract* because it is not tied to the sensorimotor specifics of a task and thus *generalizable* because the DV formed for a task with a particular sensorimotor specifics can be utilized to guide the performance in other tasks with different sensorimotor specifics, as long as the DV carries the information that is shared across those tasks.

Due to its abstract and generalizable nature, the DV space has been considered a paragon of the cognitive mind's ability to construct goal-directed mental playgrounds for intelligent behavior[13,14]. For this reason, extensive theoretical and empirical studies have been dedicated to elucidating the deliberate process of abstracting DVs from their sources and the commitment process of making a categorical choice[1,3,15-26]. These efforts substantially advanced our understanding of the deliberation and commitment processes of decision-making, including the origins of suboptimal DV encoding[27-29] and the speed-accuracy tradeoff during DV formation[30-33].

In stark contrast, much less effort has been put into understanding the cognitive processes that occur after DVs are encoded. There are good reasons to believe that these post-encoding processes are crucial in fostering adaptive behavior. Since only task-essential—but not inessential—elements are selectively integrated into DVs, DVs contain a compact form of information about the otherwise almost infinitely complex environment[34]. In this sense, the DV space can be considered a complexity-reduced space where cognitive operations can be efficiently deployed to access the task-essential information with minimal computational cost[35]. In addition, since the DV space can embed a continuous manifold like other representational spaces (i.e., sensory and motor spaces), a specific probability distribution (belief) over DV states can be formed within the DV space. This raises the possibility that a belief about DV can be used to signify the degree of uncertainty, such as 'decision confidence[36,37],' or updated over time to take advantage of stability in the environment[38]. Certainly, such computations are known to occur in the sensory and motor spaces. However, although this line of reasoning suggests that probabilistic computations are likely to be actively carried out in the DV space to steer adaptive behavior, this possibility has yet to be empirically validated.

As one potential adaptive operation in the DV space, we considered the cognitive act of committing to a decision with varying levels of granularity. A decision commitment with a specific level of granularity corresponds to confining the belief about the DV state within a specific region in the DV space. Suppose you are asked to sort the apples on a farm by size. To perform this task, you need to form a DV by calculating the size quantile of an apple: the probability that a specific apple is larger than any other apple on the farm. When asked to sort the apples into 'small' or 'large' classes, you are making decisions with a granularity of 2 (Fig. 1a, top). Here, committing to the 'small' choice corresponds to restricting your current belief about the DV state within the lower half of the range (DV = [0, 1/2]; Fig. 1b, top left). Importantly, the same commitment to the 'small' choice would have a different consequence

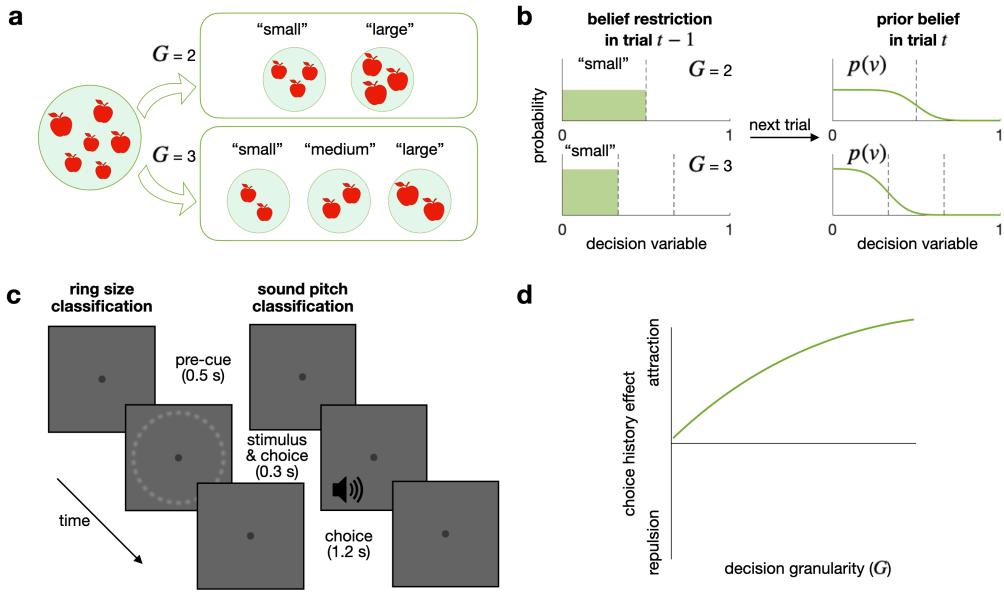

Figure 1 | Decision granularity and its hypothetical impact on subsequent decision-making. a, Decision commitment with varying levels of granularity (G). As the number of size classes into which apples are sorted increases, people are required to commit to a decision with higher G. **b,** Belief restriction by decision commitment (left) and prior updating in a subsequent trial (right) in the DV space. The higher the level of granularity is, the more restricted and stronger the prior belief is. **c,** Schematic illustrations of the ring size and sound pitch classification tasks. After viewing a ring (or listening to a sound), participants classified its size (or its pitch) into one of multiple classes. **d,** Modulation of the choice-attraction bias by decision granularity. The granularity-dependent belief updating process depicted in **b** implies that the choice-attraction bias increases with the level of granularity.

when asked to perform a ternary decision-making task with a granularity of 3 (Fig. 1a, bottom). Here, your belief about the DV state is restricted within the lowest third of the range (DV = [0, 1/3]; Fig. 1b, bottom left). From this example, one can readily intuit that once a decision is committed, the width of DV belief narrows down linearly with the granularity. Critically, if humans adaptively use their current belief as a prior expectation for future decision-making[39,40] in the DV space—as they do in the sensory space[41-47], the connection between decision granularity and belief width has a significant implication on temporal dependencies in decision-making[48]. Specifically, such belief propagation in the DV space implies that as the granularity in the current episode increases, the DV state in that episode will exert a stronger attraction on the future episode's DV state. This is because a narrower posterior in the current episode leads to a narrower prior in the next episode (Fig. 1b), which more strongly attracts the likelihood function of DV. Consequently, as the current decision becomes more granular, it is increasingly likely to be repeated in the future (Fig. 1d).

To verify this implication, we crafted an experimental paradigm in which human individuals had to commit to a range of abstract values in the DV space with varying degrees of decision granularity. As implied, we found that the attractive bias toward the previous decision becomes stronger as decision granularity increases, a phenomenon we will call the "granularity effect." Reflecting the *abstract* nature of DVs, the granularity effect was unaffected by the modality of sensory input and the arrangement of motor output, consistently observed regardless of whether the stimuli were visual or auditory and whether the choice-to-action mapping was rearranged. Reflecting the *generalizable* nature of DVs, the granularity effect was observed even when decision commitment was followed by different sensorimotor specifics, such as point estimation, as long as the following task needs to be performed in the same DV space.

Furthermore, reflecting the *independence* of the DV space from the sensory space, the granularity effect was no longer observed when decision commitment was followed by a task that only required accessing the sensory space but not the DV space. Lastly, by building a Bayesian network model[39,46,49,50], we offer a principled account of the observed granularity effect by demonstrating that it can arise from the adaptive belief propagation over sequential episodes in the abstract and generalizable DV space.

Our findings reveal a previously unrecognized adaptive process in the DV space. This highlights the human intellect's adeptness in adapting probabilistic belief distributions to recent experiences within the abstract and generalizable DV space, where task-essential information is represented concisely.

Results

Task paradigm and rationale to probe the granularity effect

To probe the granularity effect in the DV space, we asked participants to perform magnitude classification tasks[46,49-51] where the number of classes varied (2, 4, or 8) either block-wise or trial-wise. In each trial, participants viewed a stimulus and sorted its magnitude (e.g., size or pitch) into one of the pre-designated classes (Fig. 1c). Across trials, magnitudes were randomly sampled from a single fixed distribution for a given type of magnitude. By doing so, the stimulus factor (S) and the granularity factor (G) were orthogonally manipulated.

We assume that decision-makers carry out the magnitude classification task using the following algorithm: (i) they embed a single line manifold of relative magnitude[52]—a relative position within a population of interest—within the DV space, and (ii) they commit to a specific class by picking a subsection of the manifold where the item of interest falls. We then hypothesize that an act of making a decision commits the decision-maker to a specific belief about the DV states. This limits the probability distribution to the subsection of the manifold linked to the chosen class within the DV space (Fig. 1b, left). We further hypothesize that this *limited* posterior belief in the current trial propagates into the next trial, serving as a prior belief about the DV states (Fig. 1b, right) by pulling the likelihood belief given the sensory evidence in that trial, leading to the attraction bias in choice history effect: currently chosen classes are likely to be similar to previously chosen classes. Critically, the hypothesized scenario predicts that this choice-attraction bias becomes stronger as granularity increases—the granularity effect (Fig. 1d). This is because decision commitments with finer granularity result in narrower priors, which in turn exert stronger influences on DV formation.

To test this prediction, we assessed the coefficient of an interaction term involving previous choice and previous granularity ($c_{t-1} \times G_{t-1}$) in the multiple linear regression model, where the current choice (c_t) is regressed onto multiple regressors (Eq. 1; Methods). Based on previous studies, the other regressors were carefully chosen to address potential confounds. The previous stimulus (s_{t-1}) was included because it is correlated with the previous choice and tends to repel the current choice[46,53-55]. In addition, the interaction terms involving response time ($c_{t-1} \times RT_t$; $c_{t-1} \times RT_{t-1}$) was included because response time is correlated with task difficulty, which in turn is likely to covary with granularity, and can modulate the attraction effect of the previous choice on the current choice[55-58].

With the paradigm described above, we probed the granularity effect under diverse settings to ascertain whether belief propagation over decision episodes exhibits the essential characteristics of the DV space—being abstract, generalizable, and separate from sensory and motor spaces.

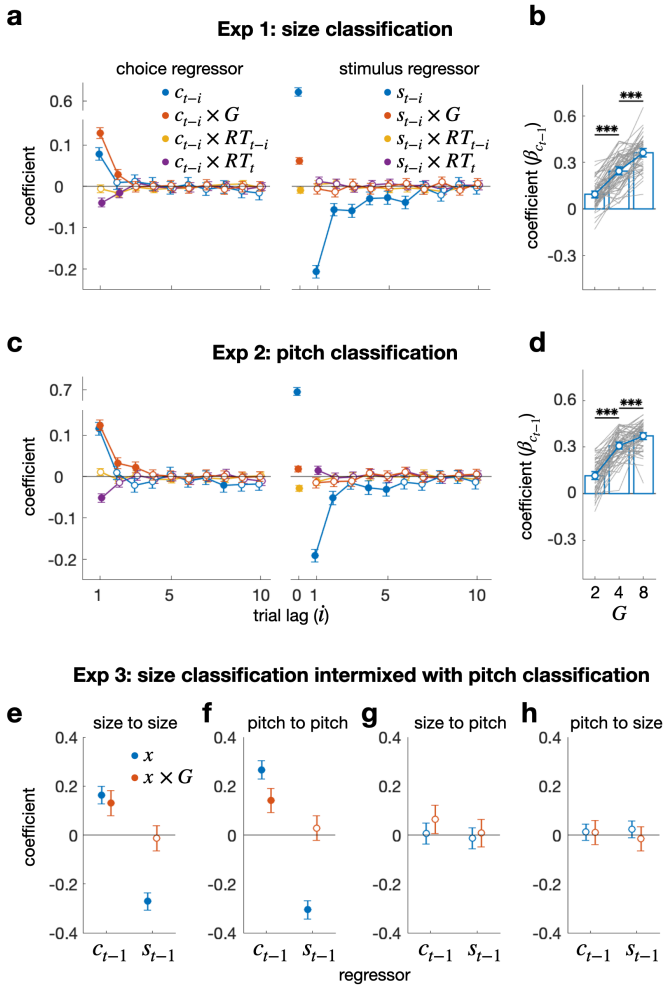

Figure 2 | Results of Exp 1, 2, and 3. a,b, Results of Exp 1. **a,** Regression of the current choice onto the multiple factors involving the previous choices (left) and the previous stimuli (right) in the size classification task. $x \times y$ denotes the interaction term between variables x and y. Here and thereafter, unless specified otherwise, the confidence interval denotes a 95% bootstrap confidence interval, and the filled circles indicate the coefficients that significantly deviate from 0 after being controlled for FDR. **b,** Regression of the current choice onto the previous choice without interaction terms, done separately for each granularity level and each individual participant. The gray lines and bars represent the individual data and group averages. The three asterisks indicate that the p-value of the pairwise t-test is less than 0.001. **c,d,** Results of Exp 2. The regression coefficients for the pitch classification task are shown using the same formats used in **a** and **b**. **e-h,** Results of Exp 3. The coefficients of the previous stimulus (s_{t-1}) and choice (c_{t-1}) factor and their interaction terms involving the granularity factor ($s_{t-1} \times G$; $c_{t-1} \times G$) are shown separately for four task-sequence conditions: when the size classification-task trial was followed by the size classification-task trial (**e**); when the pitch classification-task trial was followed by the pitch classification-task trial (**f**); when the size classification-task trial was followed by the pitch classification-task trial (**g**); when the pitch classification-task trial was followed by the size classification-task trial (**h**). The filled circles indicate the coefficients that significantly deviate from 0 after being controlled for FDR.

Exp 1-3: Modality-invariant, yet source-selective, modulation of the choice-attraction bias by granularity

We began by confirming the existence of the granularity effect in the visual domain for an adequate number of participants. In the first experiment (Exp 1), fifty-eight participants were tasked to sort a sequence of ring stimuli by size into discrete classes, a method proven effective in studying history effects

in our previous research[46,49-51]. The results of the multivariate linear regression confirmed the history effects found in previous research. The previous choice and stimulus attracted and repelled, respectively, the current choice ($\beta_{c_{t-1}} = 0.078$ ($p_{FDR} < 10^{-4}$), $\beta_{s_{t-1}} = -0.21$ ($p_{FDR} < 10^{-4}$); blue dots in Fig. 2a), as reported previously[42,46,55]. The previous choice's tendency to attract the current choice ('choice-attraction bias') became stronger as response time became shorter ($\beta_{c_{t-1} \times RT_t} = -0.040$ ($p_{FDR} < 10^{-4}$); purple dots in Fig. 2a left), as reported by Urai et al. (2019).

Importantly, the granularity effect, a phenomenon of interest and novelty, was significant ($\beta_{c_{t-1} \times G_t} = 0.13$ ($p_{FDR} < 10^{-4}$); the leftmost solid red dot in Fig. 2a left): as granularity increased, the choice attraction bias increased. The granularity effect was robust even when the previous choice effect was estimated for each granularity and each participant, respectively (Fig. 2b, $t = 11.87$ ($p = 4.94 \times 10^{-17}$) between G is 2 and 4; $t = 8.33$ ($p = 1.96 \times 10^{-11}$) between G is 4 and 8; pairwise t-test). By contrast, such a modulatory effect of granularity was absent for the tendency of the previous stimulus to repel the current choice ('stimulus-repulsion bias'; $\beta_{s_{t-1} \times G_t} = -0.0061$ ($p_{FDR} = 0.56$); the leftmost empty red dots in Fig. 2a right). This selective modulation of the choice attraction bias by granularity is consistent with our hypothesis in that the belief propagation constrained by granularity occurs in the DV space, which is *separate from* the sensory (stimulus representation) space.

Another important characteristic of the DV space is its independence from the sensory sources that form DVs—*abstractness*. This implies that the granularity effect should occur regardless of sensory modality specifics as long as decision commitment occurs in the DV space. To verify this implication, we conducted the second experiment (Exp 2), where the same fifty-eight individuals who participated in Exp 1 performed a sound pitch classification task (Fig. 1c, right). This task had the same structure as the ring size classification task, except that auditory stimuli were sorted by their pitch. As implied, granularity significantly modulated the choice-attraction bias in the pitch task ($\beta_{c_{t-1} \times G_t} = 0.12$ ($p_{FDR} < 10^{-4}$); the leftmost solid red dot in Fig. 2c left; Fig. 2d, $t = 12.04$ ($p = 2.71 \times 10^{-17}$) between G is 2 and 4; $t = 4.11$ ($p = 1.26 \times 10^{-4}$) between G is 4 and 8; pairwise t-test). It is noteworthy that the coefficients of the multivariate linear regression in the pitch task ($\beta_{c_{t-1}} = 0.12$ ($p_{FDR} = 10^{-4}$), $\beta_{s_{t-1}} = -0.12$ ($p_{FDR} = 10^{-4}$), $\beta_{c_{t-1} \times RT_t} = -0.052$ ($p_{FDR} = 10^{-4}$), $\beta_{s_{t-1} \times G_t} = -0.015$ ($p_{FDR} = 0.056$)) were strikingly similar to the corresponding values in the size task (compare Fig. 2c,d to Fig. 2a,b).

We account for the choice-attraction bias based on the belief propagation in the DV space. This account has a rational basis: it leverages the statistical tendency that magnitudes sampled closely in time from the same population are similar to one another in the natural environment[38]. For instance, the temperatures show greater similarity from one day to the next than from one week to the next. Importantly, this environmental stability holds *true only when magnitudes are sampled from the same population*. There is no reason to believe that a magnitude sampled at time t from population A is similar to a magnitude sampled at time $t + 1$ from population B, as long as there is no relationship between the two populations. For instance, as we walk in the woods, the relative pitch of bird chirping sounds I hear now does not provide any indication of the size of rocks I will encounter next. This implies that there should be no choice-attraction bias and, therefore, no granularity effect between choices of different magnitude populations if the bias reflects the brain's rational strategy to exploit environmental stability. We verified this implication in the third experiment (Exp 3), where the size and pitch tasks were randomly intermixed across trials. The choice-attraction bias and its modulation by granularity were both observed only when the same task was performed in consecutive trials (size to size: $\beta_{c_{t-1}} = 0.16$ ($p_{FDR} = 10^{-4}$), $\beta_{c_{t-1} \times G_t} = 0.13$ ($p_{FDR} = 10^{-4}$); pitch to pitch: $\beta_{c_{t-1}} = 0.27$ ($p_{FDR} = 10^{-4}$), $\beta_{c_{t-1} \times G_t} =$

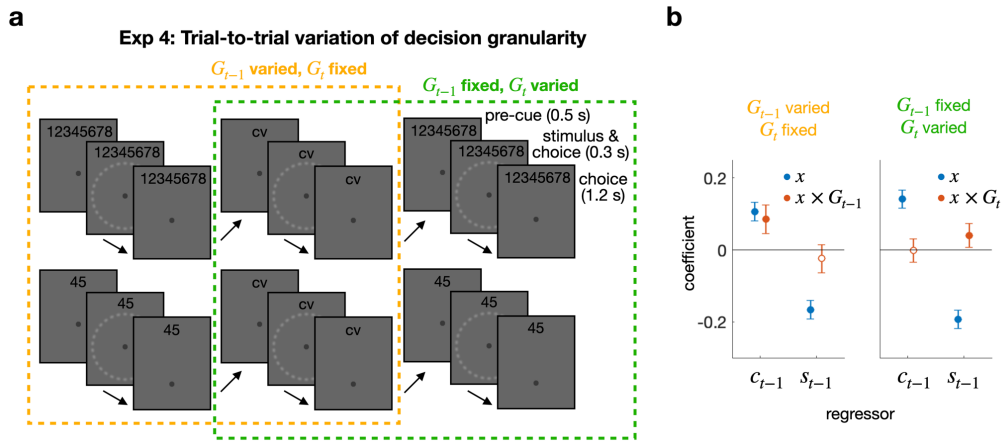

Figure 3 | Results of Exp 4. a, Experimental design. Exp 4 involved two types of blocks: one in which the level of granularity switched between 2 and 8 from trial to trial (top panels), and the other in which the level of granularity remained constant at 2 across trials (bottom panels). The decision granularity and response keys to be used were indicated by a string of numbers or letters shown at the top of the display. By sorting trials from the two types of blocks, we compared the history effects between two conditions: one in which the level of granularity was varied in the previous trial and fixed in the current trial (orange dashed box), and the other in which the level of granularity was fixed in the previous trial and varied in the current trial (green dashed box). **b**, Regression results. The coefficients of the previous stimulus (s_{t-1}) and choice (c_{t-1}) factor and their interaction terms involving the granularity factor ($s_{t-1} \times G$; $c_{t-1} \times G$) are shown separately for the two granularity-sequence conditions defined in **a**. The filled circles indicate the coefficients that significantly deviate from 0 after being controlled for FDR.

0.14 ($p_{FDR} = 10^{-4}$); Fig. 2e,f) but both not when the tasks alternated between consecutive trials (size to pitch: $\beta_{c_{t-1}} = -0.006$ ($p_{FDR} = 0.83$), $\beta_{c_{t-1} \times G_t} = 0.064$ ($p_{FDR} = 0.09$); pitch to size: $\beta_{c_{t-1}} = 0.013$ ($p_{FDR} = 0.76$), $\beta_{c_{t-1} \times G_t} = 0.011$ ($p_{FDR} = 0.76$); Fig. 2g,h). These results indicate that the belief propagation within the DV space only occurs when DVs are formed from the same source, i.e., the same distribution of task-relevant property.

Exp 4: Trial-to-trial prospective modulation of the choice-attraction bias by granularity

Until now, the granularity effect has only been demonstrated under experimental conditions where granularity varies block-wise but remains fixed trial-wise. In the fourth experiment (Exp 4), granularity was varied on a trial-to-trial basis because manipulating granularity trial-to-trial allows for putting our account of the granularity effect to a rigorous test by validating its prediction regarding the temporal direction of the effect. According to our account, the extent to which the current choice is attracted toward the previous choice is determined by the level of belief granularity in the previous trial but not in the current trial. This implies that the current choice is regressed significantly onto the previous choice × previous granularity term ($c_{t-1} \times G_{t-1}$) but not significantly onto the previous choice × current granularity term ($c_{t-1} \times G_t$).

The results confirmed this implication: the choice-attraction bias increased as the previous granularity increased, with a fixed current granularity ($\beta_{c_{t-1} \times G_{t-1}} = 0.085$ ($p_{FDR} < 10^{-4}$)), but did not increase as the current granularity increased, with a fixed previous granularity ($\beta_{c_{t-1} \times G_t} = -0.0013$ ($p_{FDR} = 0.93$)) (Fig. 3). These results indicate that what contributes to the granularity effect is not the decision granularity in the current trial but the decision granularity in the previous trial.

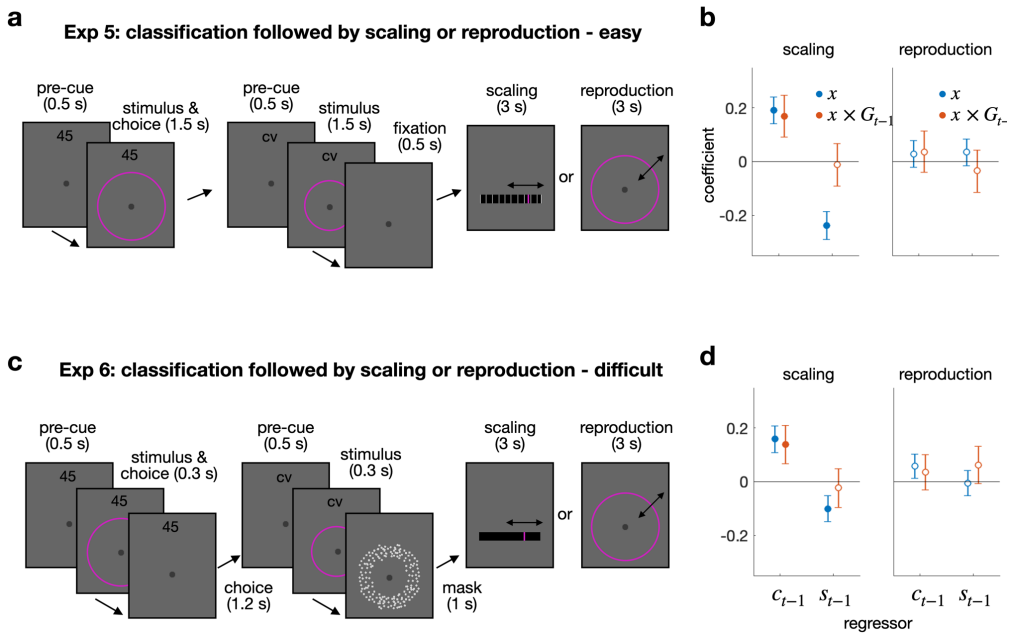

Figure 4 | Results of Exp 5 and 6. a,c, Experimental design. There were two types of blocks: the classification-task trial was followed (i) by the scaling-task trial and (ii) by the reproduction-task trial. The level of granularity was varied between 2 and 8 for the classification task. Exp 5 (**a**) and 6 (**c**) had the same design, except for differences in stimulus duration, the presence of a backward mask, and the inclusion of scaling ticks. **b,d,** Regression results. The coefficients of the previous stimulus (s_{t-1}) and choice (c_{t-1}) factor and their interaction terms involving the granularity factor ($s_{t-1} \times G_{t-1}$; $c_{t-1} \times G_{t-1}$) are shown separately for the two block types described in **a** and **c**. The filled circles indicate the coefficients that significantly deviate from 0 after being controlled for FDR.

Exp 5, 6: Generalizability and separability of the granularity effect

The belief formed in a given DV space is *generalizable* within that space but *separable* from the sensory space where stimulus features are represented. In the current context, *generalizability* implies that the belief granularized through decision commitment should continue to influence the belief formed in the next trial, even if the sensorimotor specifics in the next trial are different from those in the previous trial, as long as the next task is carried out in the same DV space as the previous task. On the other hand, *separability* implies that the granularized belief in the previous trial should NOT influence the belief in the next trial, even if the same type of sensory stimuli is used in the following trial, as long as the next task is carried out in the sensory space rather than in the DV space. We tested these two implications in the fifth (Exp 5) and sixth (Exp 6) experiments.

Specifically, the size classification task was followed randomly by either a size scaling task or a size reproduction task (Fig. 4a). Size magnitudes were randomly sampled from the fixed distribution, as before, while the number of classes varied between two and eight in the classification task to manipulate granularity. In the scaling task, observers estimated the relative size on a scale from 0 to 1. This task requires accessing the same DV space used in the classification task, where DVs are abstracted from placing perceived sizes within the overall population distribution of size. By contrast, the reproduction task, in which observers reproduce the absolute size of the ring, does not require accessing the DV space at all; instead, it can be carried out by accessing the value encoded in the sensory space. This contrast in task structure predicts that the granularity in the previous classification-task trial selectively affects the choice-attraction bias in the subsequent trial of the scaling task, but not in the reproduction task.

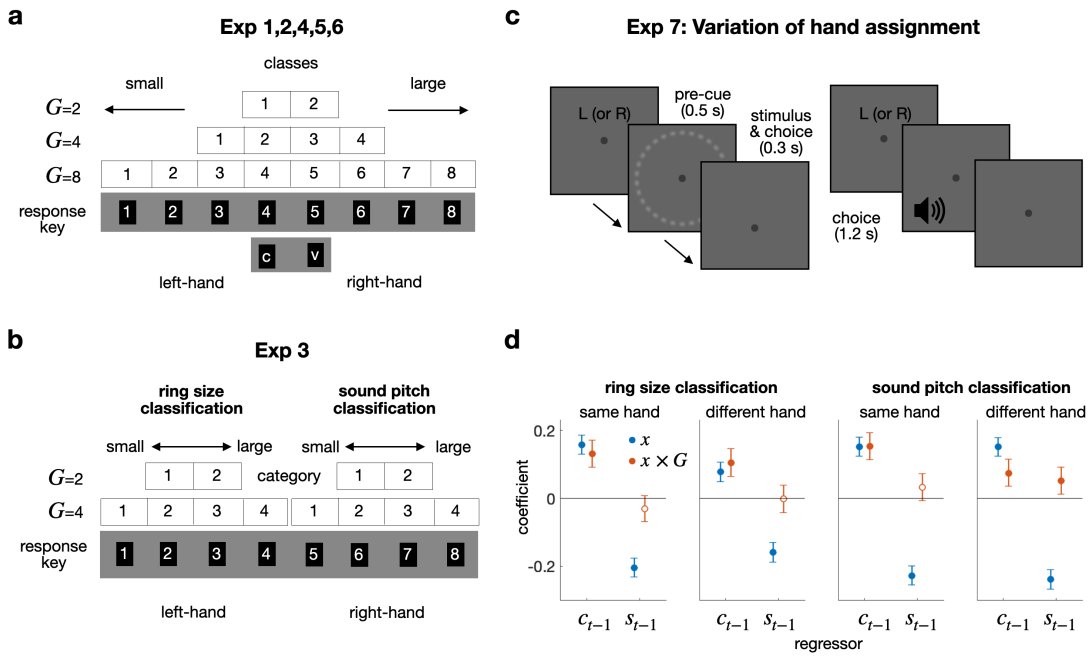

Figure 5 | Results of Exp 7. a,b, Spatial arrangement of response keys for Exp 1-6. **a,** Linear association between the class states and the locations in action space in Exp 1, 2, 4, 5, 6. Within these experiments, the class identities were orderly mapped onto a fixed set of response keys arranged on the computer keyboard, which served as a constant action space. **b,** Nonlinear association between the class states and the locations in action space in Exp 3. Within each task type, the class identities were orderly mapped onto the fixed action space, while the action space differed between the two task types since the left and right hand were used for the ring size classification (left) and sound pitch classification (right) tasks, respectively. **c,d,** Experimental design and results of Exp 7. Participants performed the ring size classification task and the sound pitch classification task in different blocks. Hand assignment was randomized from trial to trial. Participants were instructed which hand to use for a response by the letter displayed at the top of the screen at the beginning of each trial (**c**).There were four types of two consecutive trials: (i) 'same-hand ring-size-classification' trials, (ii) 'different-hand ring-size-classification' trials, (iii) 'same-hand sound-pitch-classification' trials, (iv) 'different-hand sound-pitch-classification' trials. **d**, Regression results. The coefficients of the previous stimulus (s_{t-1}) and choice (c_{t-1}) factor and their interaction terms involving the granularity factor ($s_{t-1} \times G_{t-1}$; $c_{t-1} \times G_{t-1}$) are shown separately for the four consecutive-trial types. The filled circles indicate the coefficients that significantly deviate from 0 after being controlled for FDR.

The prediction was confirmed: the scaling estimates were attracted toward the previous classification choice, with the degree of attraction increasing as granularity increased ($\beta_{c_{t-1}} = 0.19$ ($p_{FDR} < 10^{-4}$); $\beta_{c_{t-1} \times G_{t-1}} = 0.17$ ($p_{FDR} = 4.5 \times 10^{-4}$)), whereas the reproduction estimates were not influenced by the classification choice at all ($\beta_{c_{t-1}} = 0.029$ ($p_{FDR} = 0.44$); $\beta_{c_{t-1} \times G_{t-1}} = 0.036$ ($p_{FDR} = 0.49$)) (Fig. 4b). This marked difference between the two tasks was robust: it held true when stimuli were shown briefly and followed by a backward mask (Fig. 4c,d; scaling task: $\beta_{c_{t-1}} = 0.16$ ($p_{FDR} < 10^{-4}$); $\beta_{c_{t-1} \times G_{t-1}} = 0.14$ ($p_{FDR} = 4.5 \times 10^{-4}$); reproduction task: $\beta_{c_{t-1}} = 0.058$ ($p_{FDR} = 0.058$); $\beta_{c_{t-1} \times G_{t-1}} = 0.036$ ($p_{FDR} = 0.39$)). These results suggest that the act of decision commitment narrows down the range of belief about the DV states and that this reduction has a generalizable impact on tasks that access the same DV space with different sensorimotor specifics but does not affect tasks that access only the sensory space, which is separate from the DV space.

Exp 7: Action-space-invariant modulation of the choice-attraction bias by granularity

For two reasons, one might consider the action space as an alternative to the DV space for the origin of the granularity effect. First, the number of available actions increases as granularity increases (Fig. 5a). This transformation of the action space, often called 'action space shaping,' is known to affect how agents learn a task, similar to reward shaping[59]. Second, in Exp 1, 2, 4, 5, and 6, committing to a specific choice perfectly aligns with taking action at a specific location in the action space for a given level of granularity (Fig. 5a). This strong association between the action and DV spaces can confound the source of the granularity effect. Especially, it should be taken seriously because it is known that the location of the response hand and the semantic magnitude are automatically associated [60-63], and the granularity effect was not observed in Exp 3, where the semantic magnitude happened to be not aligned in action space. (Fig. 5b).

In the last experiment (Exp 7), we dissociated the DV and action spaces to address this issue. Specifically, the action space was divided into two subspaces as we did for Exp 3: left-hand vs. right-hand spaces. One of the two subspaces was randomly used on a trial-to-trial basis by instructing observers which subspace to act upon with a pre-cue (Fig. 5c). Differently from Exp 3, Exp 7 fixed stimulus modality within block and alternated it between blocks. We found that granularity modulated the choice-attraction bias, regardless of whether the action space was the same (size task: $\beta_{c_{t-1}\times G} = 0.13$ ($p_{FDR} < 10^{-4}$); pitch task: $\beta_{c_{t-1}\times G} = 0.15$ ($p_{FDR} < 10^{-4}$)) or different (size task: $\beta_{c_{t-1}\times G} = 0.11$ ($p_{FDR} < 10^{-4}$); pitch task: $\beta_{c_{t-1}\times G} = 0.074$ ($p_{FDR} = 0.0014$)) between two consecutive trials (Fig. 5d). Based on these results, we conclude that the granularity effect cannot be ascribed to either action space shaping or commitment to the action space.

A Bayesian account of the history effects in reproduction, scaling, and classification tasks

Led by the idea that human decision-makers not just form abstract representations in the DV space but also granularize and propagate them over sequential episodes there, we have conducted the seven experiments that demonstrated its implications. Next, we aim to provide a principled and unified account of the array of history effects observed in those experiments by translating this idea into a mathematical algorithm using Bayesian formalism[64-67]. These history effects can be summarized comprehensively by the 12 regression coefficients that capture how the four history factors in the previous classification-task trial—(i) choice (c_{t-1}), (ii) modulatory granularity-on-choice ($c_{t-1} \times G_{t-1}$), (iii) stimulus (s_{t-1}), and (iv) modulatory granularity-on-stimulus ($s_{t-1} \times G_{t-1}$) factors—influence the current responses in the three tasks—(i) reproduction, (ii) scaling, and (iii) classification tasks (Fig. 6a). Thus, a valid model should be capable of simultaneously capturing all these 12 observed coefficients with a single set of parameters.

As a principled account, our modeling adopted the Bayesian framework. Our central hypothesis is that beliefs are formed and updated separately, in parallel, within the stimulus space and the DV space. To implement this hypothesis within the Bayesian framework, we assumed that the stimulus and DV spaces have their own generative models where a stimulus measurement (m^s) is stochastically generated from the stimulus variable (s) in the stimulus space while a DV measurement (m^v) is stochastically generated from the DV (v) in the DV space (Fig. 6b). Consequently, two independent prior beliefs can propagate across trials in parallel within the stimulus and DV spaces. This parallelism in belief propagation between the two separate representational spaces is key to explaining why and how the

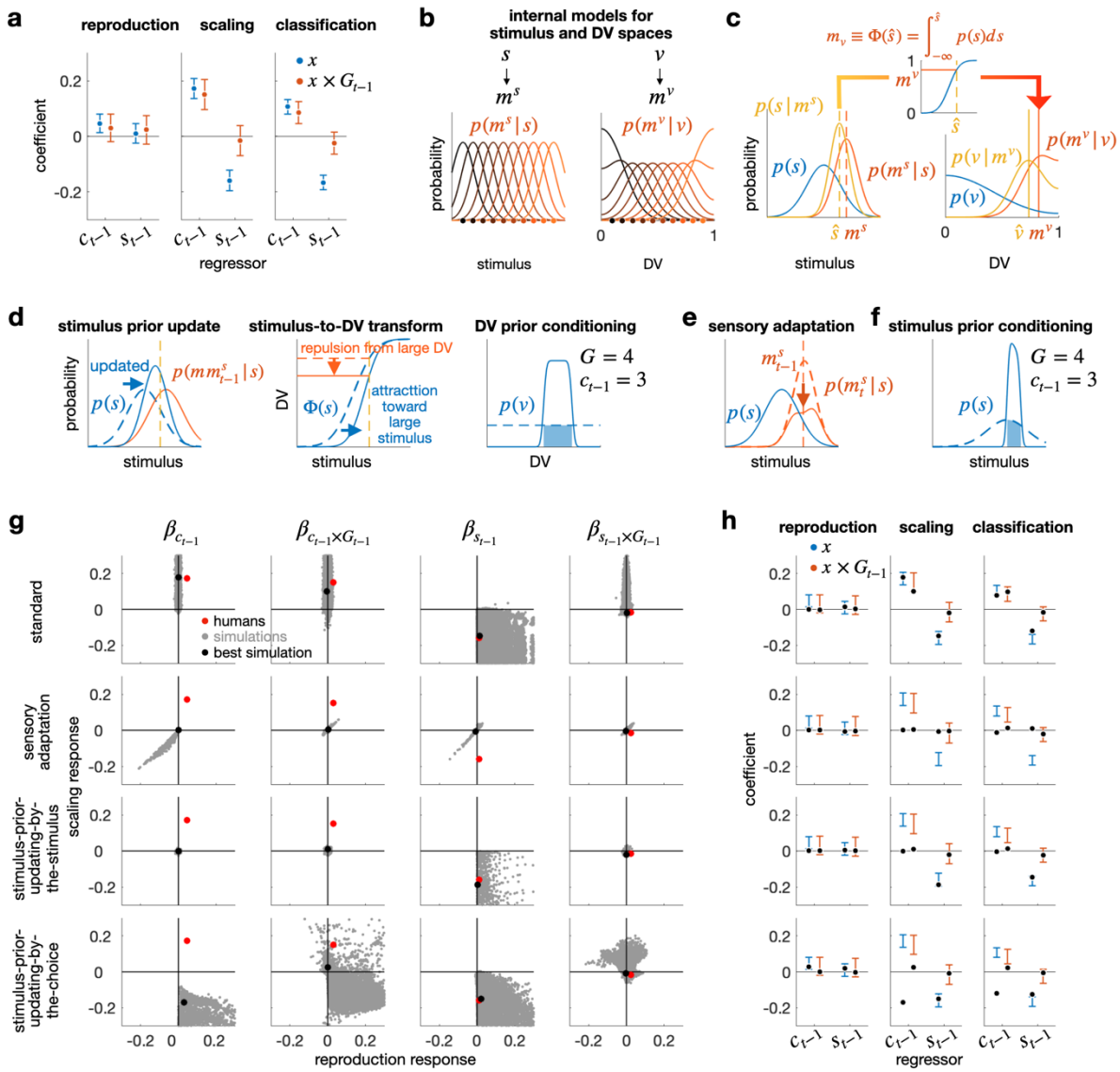

Figure 6 | Results of the model simulations. a, Benchmark history effects to be explained. Seeking a principled and unified account of the history effects found in the current study, we focused on the impacts of the previous choice (c_{t-1}) and stimulus (s_{t-1}), as well as their interaction with the previous granularity level ($c_{t-1} \times G_{t-1}$ and $s_{t-1} \times G_{t-1}$) on the current response for each of the three tasks: reproduction, scaling, and classification. Specifically, the regression coefficients found in the combined data from Exp 5 and 6 were used for the reproduction and scaling tasks, while those from Exp 4 were used for the classification task. Any successful account should simulate these 16 regression coefficients. The error bars correspond to the 95% bootstrap confidence intervals. **b,** Internal models for stimulus and DV spaces. In the stimulus space, given a specific state of the stimulus variable s, a sensory measurement of the stimulus m^s is stochastically generated to form a likelihood function centered around the true state of s (left panel). In the DV space, given a specific state of the DV s, an internal measurement of the DV m^v is stochastically generated to form a bounded ($[0, 1]$) likelihood function centered around the true state of v (right panel). **c,** Inferences in stimulus and DV spaces. The state of the stimulus variable is inferred given m^v as $\hat{s}$ according to Bayes rule with the internal model described in **b** (left panel). The stimulus estimate in the stimulus space $\hat{s}$ is transformed into a DV measurement m^v, which is defined as the quantile of $\hat{s}$ given the prior belief about the stimulus $p(s)$ (middle panel). Given m^v, the state of the DV is inferred as $\hat{v}$ according to Bayes rule with the internal model described in **b** (right panel). **d,** Belief updating in the standard model (see main text). The prior beliefs are updated in parallel in both stimulus and DV spaces. The stimulus prior is updated to be attracted (from dashed to solid blue curves) toward the memory of previous stimulus (red curve) (left panel). As a result, the same stimulus estimate (vertical

dashed line) is transformed into different states of m^v before and after the updating (from dashed to solid horizontal curves and lines in the middle panel). In the DV space, the DV prior is conditioned by the previous decision commitment, with varying extents based on its granularity (from dashed to solid curves in the right panel). **e,** Changes in likelihood function in the *sensory adaptation model*. Sensory adaptation to the previous stimulus s_{t-1} leads to the distortion of the likelihood function in the current trial, which is suppressed (from dashed to solid red curves) around the previous stimulus measurement m^s_{t-1} (dashed vertical red line). **f,** Stimulus prior updating in the *stimulus-prior-updating-by-the-choice model*. Unlike the standard model, this model assumes that the stimulus prior is updated to be conditioned by the previous decision commitment, with varying extents based on its granularity (from dashed to solid curves). **g,h,** Simulation results from the standard model (top panels) and its three variants (bottom three panels). **g,** Coefficients for the regression of the reproduction and scaling responses onto the stimulus (s_{t-1}) and choice (c_{t-1}) factor and their interaction terms involving the granularity factor ($s_{t-1} \times G_{t-1}$; $c_{t-1} \times G_{t-1}$) in the previous classification-task trial. In each panel, the coefficients for the scaling-task trials are plotted against those for the reproduction-task trials: gray dots, coefficients from individual simulations with different sets of model parameters (see Methods); black dots, coefficients from the simulations with the model parameters giving the outcomes closest to the observed ones, which are indicated by the red dots. **h,** Comparison of the best simulation outcomes to the observed ones. The confidence intervals for the human data depicted in **a** are juxtaposed with the regression coefficients for the model simulations with the best parameters (black dots).

stimulus-repulsion and the choice-attraction biases occur in both scaling and classification tasks but not in the reproduction task, as elaborated below.

From these two generative models, normative inference processes are derived to perform the three tasks (Fig. 6c). The inferential processes have three modules: the s-space module, where beliefs about stimulus states (e.g., absolute magnitudes of size) are formed and updated (the left panel of Fig. 6c); the v-space module, where beliefs about DV states (e.g., probability of being larger than others in size) are formed and updated (the right panel of Fig. 6c); and the s-to-v transformation module, which nonlinearly maps beliefs about the stimulus states to the DV states using the cumulative distribution function of the stimulus prior (Φ) (the center panel of Fig. 6c). With these modules, the three tasks are carried out as follows. The reproduction task is carried out within the s-space module because it requires inferring the absolute magnitude of a stimulus, which is obtained by calculating the maximum a posteriori (MAP) of stimulus ($\hat{s} = \arg\max_s p(s|m^s)$) based on the stimulus prior $p(s)$ and likelihood function $p(m^s|s)$ (the left panel of Fig. 6c). Then, m^v (the DV measurement) results from the s-to-v transformation, via which the inferred state of the stimulus $\hat{s}$ is mapped onto the DV space. The scaling and classification tasks are both carried out in the v-space module because they require inferring the relative magnitude of a stimulus, the DV. For the scaling task, a point estimate of DV is obtained by calculating the MAP of DV ($\hat{v} = \arg\max_v p(v|m^v)$), which involves combining the DV prior $p(v)$ and likelihood function $p(m^v|v)$ in the v-space module (the right panel of Fig. 6c). For the classification task, the DV space is evenly discretized according to the granularity, and a class is chosen as the order of the discretized range where $\hat{v}$ is located.

In what follows, we provide an intuitive account of how our model can predict the history effects observed in the three tasks. As our group previously proposed[46,49,50], we posit that when a stimulus is observed, the stimulus prior $p(s)$ is updated to be attracted to the memory of that stimulus (mm^s) (left panel of Fig. 6d). Because of this update in $p(s)$, the transformation function is also attracted toward the previous stimulus. In turn, this attracted transformation function causes the DV in the subsequent trial to be repelled away from the previous stimulus (center panel of Fig. 6d). Thus, the larger the previous stimulus, the smaller the current DV measurement, and the more the current response is repulsed away from the previous stimulus. This explains the stimulus-repulsion bias ($\beta_{s_{t-1}} < 0$) observed in both classification and scaling tasks (the right two panels of Fig. 6a) while it does not induce the stimulus-

repulsion bias in reproduction task because what is repelled is not the stimulus itself but a DV measurement (left panel of Fig. 6a). Furthermore, it does not induce any granularity effect on the stimulus-repulsion bias because the granularity was not incorporated into the stimulus prior updating.

As for the choice-attraction bias and granularity effect, we posit that when a decision is made, the posterior belief of DV is narrowed down to match the range of DV that the decision commits to. This belief is then carried over into the future, serving as the DV prior in the next trial (right panel of Fig. 6d). Thus, the more granular the previous decision, the narrower the current DV prior, and the more the current response is attracted to the previous decision. This explains the choice-attraction bias ($\beta_{c_{t-1}} > 0$) and the granularity effect ($\beta_{c_{t-1} \times G_{t-1}} > 0$) in both classification and scaling tasks (the right two panels of Fig. 6a). In the reproduction task, neither the choice-attraction bias nor the granularity effect occurs (the left panel of Fig. 6a), as what is granularized is the DV space, while an estimate of size magnitude does not require accessing the DV space.

To confirm our intuitive account, we conducted model simulations[50,68] using a range of model parameters that were deemed reasonable based on participants' performance in Exp 4-6 (see Methods). We quantified the history effects using multiple regression, following the same procedure as with human participants. The simulated regression coefficients show that our model's behavior (the gray dots in the top panel of Fig. 6g) can display the pattern of history effects that are similar to those observed for human participants (the red dots in the top panel of Fig. 6g). When the best model parameters were selected, the pattern of historical effects showed remarkable similarity between the model and human data (as the black dots in the top panel of Fig. 6h).

Falsification of alternative accounts of the observed history effects

Having confirmed our model's capability to produce the observed history effects, we now investigate whether these effects can be produced by alternative scenarios that do not necessarily entail creating the DV space and propagating beliefs across episodes there, which is central to our explanation of the observed history effects.

First, we considered the 'sensory-adaptation' hypothesis as an alternative scenario to the 'stimulus-prior-updating' of our model in explaining the stimulus-repulsion bias. This hypothesis posits that the previous stimulus reduces the sensory apparatus's encoding gain, potentially causing the current perception to be repelled away against the previous stimulus[43,69,70]. We incorporated the 'sensory-adaptation' scenario into our Bayesian model by modifying the stimulus likelihood function[71] (as shown in Fig. 6e; see Methods for details). This scenario can generate the stimulus-repulsion bias in the scaling task ($\beta_{s_{t-1}} < 0$). However, whenever it does, it also generates the same bias in the reproduction task (the second row of Fig. 6g,h), which is an uncorrectable deviation from the observed effects.

Second, this failure of the 'sensory-adaptation' in capturing the repulsive bias in the scaling task indicates that the repulsive bias might originate from another mechanism. Thus, we considered the 'stimulus-prior-updating-by-the-stimulus' hypothesis (see Methods for details). This scenario can generate all history effects of the previous stimulus in the three tasks simultaneously (the symbols involving s_{t-1} on the third rows of Fig. 6g,h). Especially, it can simulate the stimulus-repulsion in the scaling and classification task without displaying the repulsive bias in the reproduction task. However, it cannot display any history effects of the previous choice (the symbols involving c_{t-1} on the third rows of Fig. 6g,h), and therefore cannot be considered a comprehensive explanation for the observed history effects.

Lastly, despite its failure in capturing the previous choice effect, the success of the stimulus-prior-updating-by-the-stimulus' hypothesis in capturing the previous stimulus effect suggests that the stimulus-prior-updating can explain the history effects if it is appropriately modified to incorporate the previous choice effect. Thus, we considered the 'stimulus-prior-updating-by-the-choice' hypothesis as a scenario that granularizes and propagates beliefs over episodes, not in the DV space, but in the stimulus space[72,73] (Fig. 6f; see Methods for details). Because it is modified from the stimulus-prior-updating-by-the-stimulus model, the stimulus-prior-updating-by-the-choice hypothesis can produce the history effects of the previous stimulus (the symbols involving s_{t-1} on the fourth rows of Fig. 6g,h). However, it still cannot produce those of the previous choice. It displays the choice-repulsion bias, instead of the choice-attraction bias, and fails to produce the granularity effect (the symbols involving c_{t-1} on the fourth rows of Fig. 6g,h). Thus, the 'stimulus-prior-updating-by-the-choice' hypothesis does not offer a comprehensive account of the observed history effects.

As we have shown earlier, when we modified the 'stimulus-prior-updating-by-the-stimulus' model by hypothesizing that belief is granularized and propagated in the DV space rather than in the stimulus space, the 12 regression coefficients were successfully captured. This success and the failure of the hypotheses to generate and produce the observed history effects support the necessity for dual belief propagations through the stimulus space and the DV space.

Discussion

The essence of human intelligence, particularly its most advanced form in comparison to other natural and artificial intelligences, lies in the ability to give abstract structure to daily experiences[74,75]. A prime example of structured abstraction in human cognition is forming DVs from limited or impoverished sources, including sensory evidence, prior knowledge, and action cost (reward) to guide decision-making with uncertainty[2,9,14]The processes involved in DV formation have been studied extensively, but the utilization of DVs after formation remains relatively unexplored despite its importance in adapting to the environment. Based on the concept that the space representing DVs is well-suited for efficiently translating past experiences into future expectations, we hypothesized that (i) when a categorical decision is made, it restricts the belief distribution about DV states to a particular range in the DV space, and (ii) this restricted belief distribution is then carried forward to future trials and used as a prior expectation for potential DV states. As an empirically testable implication of this hypothesis, we predicted the granularity effect: the choice-attraction bias—the extent to which the current choice is attracted toward the previous one—increases as the commitment to DV states becomes finer with an increasing level of decision granularity.

Confirming this prediction, human individuals reliably displayed the granularity effect. Critically, its presence and absence in our experiments suggest that it originates from the DV space. To summarize, the granularity effect: (i) *did* occur when size (pitch) classification or scaling was followed by size (pitch) classification regardless of whether different hands were used for enacting the previous and current choices; (ii) *did not* occur when size classification was followed by pitch classification, and vice versa; (iii) *did not* occur when size classification was followed by size reproduction; (iv) *did not* occur on the stimulus-repulsion bias. These results suggest that the granularity effect does not originate from the action

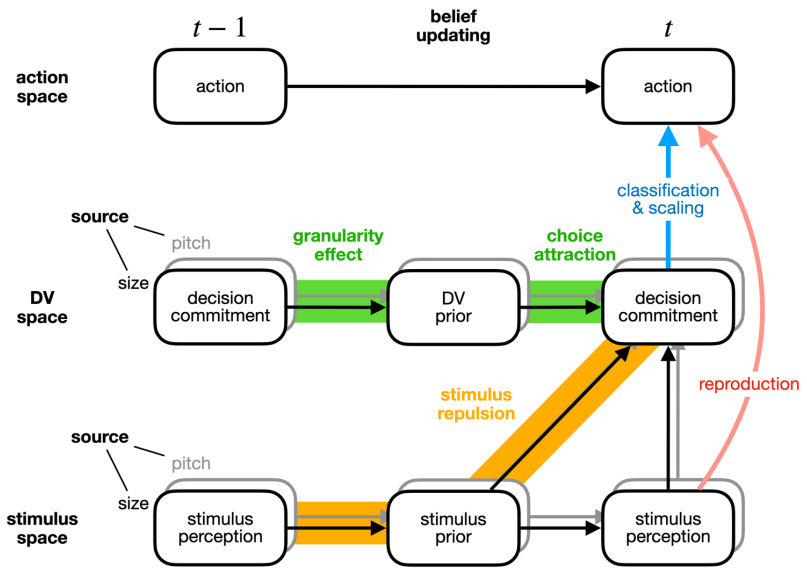

Figure 7 | Distinct routes of belief propagation for the history effects in the reproduction, scaling, and classification tasks. The cognitive acts involved in the three tasks are summarized in three layers of spaces: stimulus perception in stimulus space (bottom), decision commitment in DV space (middle), and action in action space (top). Between consecutive trials, prior beliefs are updated in parallel in both stimulus and DV space. According to our proposed standard model, the stimulus-repulsion bias originates from the route starting with stimulus perception in the previous trial, then the update of the stimulus prior, and finally the decision commitment in the current trial (arrows with yellow shades). The choice-attraction bias and its modulation by granularity (the granularity effect) originates from the route starting with the decision commitment in the previous trial, then the update of the DV prior, and finally the decision commitment in the current trial (arrows with green shades). As a result, all these history effects do occur in the scaling and classification tasks, which require accessing the DV space (blue arrow), but the granularity effect and choice attraction do not occur in the reproduction task, which does not require accessing the DV space (pink arrow).

space (i), the source-general DV space (ii), nor the stimulus space (iii and iv), but rather from the source-specific DV space (black and gray arrows with green shades in Fig. 7).

As a principled and unified account of the history effects observed under the various task conditions above, we built a Bayesian model in which probabilistic beliefs propagate over episodes in both stimulus and DV space. The model's ability to produce the observed history effects suggests that the human mind does form beliefs with varying degrees of uncertainty not just in the stimulus space but also in the DV space. Furthermore, it indicates that these beliefs are used for future purposes through probabilistic computation in the stimulus and the DV spaces in parallel.

Our findings expand the current understanding of human intelligence by showing that humans glean *generalizable* knowledge during categorical decision-making, represent it in an *abstract* continuous space that is *separate* from where sensory stimuli or motor plans are represented, and update and apply this continuous belief distribution over episodes of cognitive acts with different sensorimotor specifics to effectively adjust their behavior trial-to-trial in ever-changing environments.

Consequences of decision commitment

Previous studies on decision-making focused on how decision-makers form DVs and commit to a specific option based on their state. Signal detection theory[1] (SDT) has been instrumental in guiding research on DV formation and decision rules by defining the DV as the ratio of likelihoods of binary options and

offering a decision rule based on criterion setting. Sequential analysis theory[3,4] (SAT) adds a dynamic quality to DV formation and offers a decision rule to stop DV formation and commit to a decision. Guided by SDT and SAT, systems neuroscientists significantly advanced our understanding of decion-making by identifying neural correlates of DV state[18,76-79], dynamic DV formation[80-82], and decision commitment[16,83], despite being challenged by recent perspectives and findings (see [84,85] for extensive reviews). We took a step further by exploring the cognitive consequences of decision commitment. By examining the impact of decision granularity on future cognitive processes, we have discovered that the belief about the DV state is updated as a consequence of decision commitment and is subsequently integrated into the future formation of DV as a form of prior belief. Specifically, the granularity effect suggests that committing to a choice restricts the belief distribution to a discrete range of the DV state linked to that choice.

Why does the brain restrict the belief of DV in accordance with granularity? We conjecture that this belief restriction has a rational basis. Making a decision is a deliberate process that requires significant mental effort[86,87] and involves a hierarchy of brain regions[85,88-91], which uses up substantial neural computation and communication resources[92,93]. In addition, the quality of decisions would likely improve with an increasing amount of resources[35,94,95]. This means that as a decision becomes more granular, more resources are spent to commit (as evidenced in longer RTs; mean RTs of Exp 1: 0.65 s, 0.82 s, and 0.96 s for $G = 2, 4,$ and 8 respectively; Exp 2: 0.74 s, 0.89 s, and 1.04 s for $G = 2, 4,$ and 8 respectively). Therefore, it seems reasonable to give more weight to decisions with finer granularity, thereby reinforcing beliefs for which more resources are spent. In this sense, the granularity-dependent belief restriction of DV can be viewed as an instantiation of resource-rational computation[94,96-98].

Shaping beliefs within the decision-variable space

In the context of probabilistic knowledge[99-102], "belief" refers to a subjective knowledge of probabilistic information. Beliefs are beneficial as long as they reflect the actual states of variables and their true relationships in the environment. Therefore, a key aspect of explaining adaptive behavior is understanding how individuals form and use their beliefs to adapt to their surroundings.

Probabilistic decision theories have been offering powerful accounts of how human decision-makers carry out various sensory-motor tasks by positing that they can form nearly optimal beliefs about the state of the world (prior knowledge)[103-107], the contingency between sensory evidence and its causal state of the world (likelihood function)[108,109], and the contingency between the motor command and its outcome in the world (conditional distribution)[72,73], and the reward linked to a particular outcome (loss function)[109]. It should be stressed that these beliefs are all assumed to be formed about the states and outcomes of the concrete world, i.e., stimulus measurements or motor commands (e.g., 'motion direction and its sensory signals' or 'pointing plan and its hand location in world coordinates'). However, DVs have never been treated as a random variable with uncertainty but only as a point estimate without uncertainty[1,9,110,111]. Our simulation of different versions of the Bayesian model revealed that to display the granularity effect, the probabilistic belief in the DV space needed to be updated through decision commitment, resulting in the restriction of the belief to a specific range of the DV state corresponding to the *granulated* commitment. These results suggest that beliefs are updated in parallel, with one in the stimulus space engendering the stimulus-repulsion bias (arrows with orange shades in Fig. 7), and the other in the DV space engendering the choice-attraction bias and granularity effect (arrows with green shades in Fig. 7).

Our interpretation above raises a normative question: Why does the human brain shape probabilistic knowledge in the DV space, not just in the stimulus or action spaces? We conjecture that several points can justify such belief shaping. First, beliefs in the DV space can be more invariant to nuisances and thus be more generalizable compared to those in the stimulus or action space. For instance, the absolute size and brightness of a thing are subject to changes depending on the viewing distance and illumination, respectively. However, its size and brightness relative to those of the others in a population are tolerant to such nuisance factors. Likewise, enacting a decision in a specific part of space is subject to changes depending on the provisional contingency between choice and action policy. In such circumstances, it would be more reasonable to hold beliefs in a representational space immune to such contingencies. This makes the DV space a reliable place to store knowledge from past decision-making episodes and use it for future episodes. Second, the prior belief about stimulus distribution becomes, in principle, annulled in the DV space. This is because the DV measurements are linked to the stimulus estimate via the cumulative distribution functions of the stimulus prior belief (Fig. 6c). Suppose the stimulus estimates $\hat{s}$ follow a distribution similar to the stimulus prior $p(s)$. Then, the transformed DV measurements $m^v = \Phi(\hat{s})$ would be uniformly distributed in the DV space. Hence, the DV space needs its own prior beliefs to utilize the probabilistic information that relates past to future events in an abstract manner. Lastly, DVs contain rich, task-relevant information in a concise format because they are formed by combining multiple factors that help achieve the defined objective of the task. This makes the DV space an efficient place to form and propagate beliefs over a sequence of cognitive events. In summary, the DV space offers a general platform for shaping abstract knowledge that can be efficiently applied in various situations, even in complex environments filled with distracting factors in the stimulus and action domains.

Our Bayesian account of the granularity effect based on probabilistic computation in the DV space leads to an empirically testable prediction about the neural representation of DVs. Specifically, our account suggests that the neural signals of DVs should contain information about the uncertainty regarding the trial-to-trial states of the task-relevant DVs. Recently, human neuroimaging[112] and monkey electrophysiological[113] studies have shown that population neural activities in the primary visual cortex carry uncertainty-associated signals in the stimulus representation space (e.g., visual orientation feature). Thus, one may take a similar approach to the high-tier cortical regions where DVs are likely to be represented, such as the parietal or prefrontal cortices. We predict that their trial-to-trial population activity conveys uncertainty representations about DVs that better explain decisions than point estimate representations.

Distinguishing between the perceptual history effects arising in the stimulus and DV spaces

The phenomenon of history effect, also known as "serial dependence," has been observed in various perceptual tasks (see [114] for a comprehensive review). The most commonly reported type of history effect is the positive sequential dependence, also known as "attractive bias," where various cognitive processes, including estimation and decision-making, are biased toward recent perceptual experiences[115]. The attractive bias has been observed in two tasks: reproduction and categorization tasks. In the former, observers need to reproduce a target's feature on a continuous feature spectrum using an adjustment method[44,47,54,116-119], as was done in the 'reproduction-task' trials of Exp 5 and 6 in the current work. In the latter, observers decide which particular ordinal category a target's feature value belongs to using a

forced-choice method[55-58,120], as was done in the 'classification-task' trials of all the experiments in the current work.

It is unclear whether "attraction" arises from the same source when performing reproduction and categorization tasks[55,114,115]. In a recent review[114], the differences in history effect between the two tasks were attributed to the difference between continuum or discrete values used for reporting. However, our findings indicate that the difference in representational space is the critical distinction between reproduction and categorization tasks, which require accessing the stimulus and DV spaces, respectively. Supporting this idea, we found that the choice-attraction bias and the granularity effect were present when the classification-task trial was followed by the scaling-task trial but not when followed by the reproduction-task trial (Exp 5 and 6). This points out that the key factor in transferring past experiences into future ones is not the consistency between consecutive trials in reporting format (whether discrete or continuous), but rather the commonality of their representational space.

The other history effect observed in the current work is the stimulus-repulsion bias. Critically, similar to the choice-attraction bias, the stimulus-repulsion bias occurred when the classification trial was followed by the scaling trial but not when followed by the reproduction trial. These results help to resolve the issue about the origin of the stimulus-repulsion bias in the classification task, determining if it arises from sensory adaptation[43,69,114,121] or from updating stimulus distribution[45,46,49,50,53]. The sensory adaptation hypothesis implies that the stimulus-repulsion bias occurs regardless of whether the classification trial was followed by the scaling trial or by the reproduction trial because the key factor for sensory adaptation is the physical stimulus itself. Our findings defy this implication and suggest that updating the stimulus distribution is the source of the stimulus-repulsion bias in the classification task. This conclusion corroborates the conclusion drawn from a recent neuroimaging study of our group[46].

Potential confounds of decision granularity

We found that the granularity of the previous decision *modulates* the extent to which the current decision is biased toward the previous decision. We attributed this modulatory effect of decision granularity to the way beliefs propagate in the DV space. Could this modulation be caused by other modulatory factors that are known to influence serial dependence, such as 'stimulus uncertainty,' 'performance confidence,' and 'attention'? We are opposed to this possibility for the following reasons.

Previous studies demonstrated the modulatory influence of stimulus uncertainty on serial dependence by manipulating the orientation cardinality[41,122], spatial frequency[41,123], contrast[124], eccentricity[69], and noise[125] of visual stimuli. In our study, these stimulus parameters remained constant and, therefore, did not covary at all with decision granularity. Hence, the granularity effect is unlikely to originate from stimulus uncertainty.

While the physical properties of stimulus input objectively determine stimulus uncertainty, performance confidence subjectively varies from trial to trial[36,126]. Previous studies have shown that a higher level of performance confidence in the previous trial tends to promote serial dependence with a stronger attractive bias[127,128] and that the proxy measures of confidence, like RT and pupil size, also influence the degree of serial dependence[55-58]. However, the modulatory direction of this previous confidence is opposite to the granularity effect because, although higher levels of confidence are supposed to promote the choice-attraction bias[55,58], the RT data indicate that the level of confidence becomes lower as the level of decision granularity increases. Furthermore, even when we included the RT measurements as the modulatory factors for the influences of the previous stimuli and choices when

evaluating the granularity effect using a multiple regression model, the granularity effect could not be explained away by changes in RT from trial to trial.

In previous studies, researchers manipulated the spatial[129] and featural[130] aspects of attention, as well as the amount of attention, by instructing participants to either report or not report stimulus features[69,131]. By doing so, they showed that the attractive serial dependence increases with proper attention to the previous stimulus. This raises the question of whether the level of decision granularity was confounded with attention. However, this 'attention' scenario cannot explain why the granularity effect only occurred when the classification-task trial was followed by the scaling-task trial, and not when it was followed by the reproduction-task trial (Exp 5 and 6). If the effect were caused by attention, it should have been observed in both conditions.

The granularity effect as a novel history effect

Given the robust yet highly specific nature of the granularity effect, we conducted a thorough search of the existing literature to identify any previous mentions of comparable phenomena. To our best knowledge, a kind of sequential effect most similar to the granularity effect has been observed in a series of studies focusing on the 'absolute identification' task[132-135]. In this task, where participants needed to report the exact magnitude of a stimulus feature, the influence of the previous report on the current one tended to grow as the number of response options increased. However, this increase in sequential dependence cannot be solely attributed to the number of response options, as the number of stimuli was perfectly correlated with that of response options in the absolute identification task. When they were decorrelated in one exceptional study[133], there was no significant increase in sequential dependence as a function of response option. Newly registering the granularity effect in the list of history effects, we assert that any comprehensive account of the history effects must address the granularity effect.

Limitations

As a computational-level account[136] of the granularity effect, we proposed a Bayesian model. In this model, beliefs are formed and updated according to an internal model that assumes representational stability in the DV space. Although this model successfully captured all the history effects observed under various experimental conditions, it has limitations that need to be addressed to provide a comprehensive account of the history effects. For sure, the model needs to be extended to incorporate other decision-making tasks that may require DV spaces different from the one needed to classify stimulus ordinality, as in our experiments. Such an extension would require probing the granularity effect in alternative decision-making tasks involving a varying number of choice options, particularly those that do not depend on the order of stimuli[137-139].

Despite this need for further elaboration, our findings point to the DV space as a previously unrecognized source of trial-to-trial belief updating. We believe that future efforts to account for the across-trial belief updating processes in the DV space will significantly advance the current understanding of how the human brain efficiently adapts to its surroundings by constructing an abstract and continuous —thus highly generalizable—belief distribution out of their categorical decisions.

Methods

Participants

The study consisted of seven experiments (Exps 1-7) with 84 human participants having normal or corrected-to-normal vision and hearing. The participants took part in one or more of these experiments, as follows: 58 participants (39 females; aged 18-33 years) in Exps 1 and 2; 18 participants (11 females, aged 22-33 years) in Exp 3; 18 participants (11 females, aged 20-33 years) in Exp 4; 11 (5 females, aged 19-31 years) participants in Exp 5; 15 participants (13 females, aged 19-29 years) in Exp 6; 30 (19 females, aged 20-33 years) participants in Exp 7. Prior to participating, they all provided informed consent and were unaware of the purpose of the experiments. The experimental procedures were approved by the Research Ethics Committee of Seoul National University.

Experimental setup

Visual and auditory stimuli were displayed on a computer monitor (LG 27UL550, refresh rate of 60 Hz and resolution of 1920 x 1080 pixels) and heard through a two-channel speaker (Altec Lansing Series 100) in a dimly lit enclosed space. The viewing distance was 62 cm and enforced with a chin rest. The codes for controlling experiments, including stimulus generation and presentation, were written in Matlab (Mathworks, Inc.) in conjunction with the Psychtoolbox [140] and run on an Apple Mac Pro computer with Quad-Core Intel Xeon E5 3.7 GHz, 12 GM RAM. Manual responses were received by an i-rocks KR-6170 keyboard.

Experiment 1

Exp 1 consisted of three types of blocks: 'threshold-calibration,' 'training,' and 'testing' blocks. In the threshold-calibration blocks, participants began each trial by fixating a small dot (diameter in visual angle, 0.27°; luminance, 0.98 cd/m^2) appearing at the center of a dark screen (1.11 cd/m^2), which remained throughout the trial to help them maintain their fixation. Half a second after the fixation dot appeared, a thin (standard deviation of Gaussian envelope, 0.11°), white (1.45 cd/m^2) dashed (radial frequency, 30 cycles/360°) ring was presented for 0.3 s. Participants were required to classify the ring as 'small' or 'large' based on size within a 1.5-s decision window. We provided feedback for their choice on a trial-by-trial basis by changing the fixation dot's color for 0.5 s to green, red, or yellow, depending on whether the choice was correct, incorrect, or a miss, respectively. The correctness was determined using the class boundary set at the 3° radius. The miss trial is a trial where participants failed to respond within the decision window or pressed an undesignated button.

For each participant, a tailored threshold difference in ring size was calibrated through 4 blocks of trials, each consisting of 50 trials, using three randomly interleaved chains of one-up-two-down staircases according to the PEST rule [87], where the three chains started from the easiest, intermediate, and hardest stimuli, respectively. The first 20 trials were excluded from analysis for their instability. The cumulative normal distribution function was fit to the classification psychometric curve using a maximum-likelihood procedure. The threshold difference was defined as the ring size associated with 90 percent correct proportion based on the fitted function. Ring sizes for the training and testing blocks of trials were sampled from a normal distribution with a mean corresponding to the pre-determined boundary size (3°) and a standard deviation determined by the threshold difference.

The threshold calibration blocks were initially followed by the alternating training and testing blocks for the first 18 blocks, and then solely by the testing blocks for the remaining 12 blocks. The structure of the training and testing blocks was the same as the threshold-calibration block, except that each block had 45 trials, and the number of choice options (classification granularity) ranged from 2, 4 to 8. For each block, the classification granularity was set at a single level randomly chosen from the three levels. Participants were informed of this before the block began. The training and testing blocks differed only in that trial-to-trial corrective feedback was provided only in the former. The feedback during the training blocks resembled the threshold-calibration blocks, but with the additional feature of displaying the correct response button in incorrect and miss trials. For each participant, a total of 315 trials were acquired for each granularity level across the 21 testing blocks (9 blocks from the alternating period and 12 blocks from the non-alternating period). The trials used for data analysis were exclusively from these testing blocks.

As mentioned earlier, the ring size on each trial of the training and testing blocks was chosen randomly from a distribution based on the results of the threshold-calibration trials. For any given ring size, its class was defined by the median, quartiles, and octiles of this size distribution for the granularity levels of 2, 4, and 8, respectively. It should be noted that the size distribution remained constant throughout the entire testing and training blocks, while the classification granularity varied from block to block. This allowed us to manipulate the main variable of interest, granularity level, while controlling for any potential effects of stimulus range.

Participants indicated their choice by pressing a number key with both hands on the computer keyboard (Fig. 5a): the [4,5], [3,4,5,6], and [1,2,3,4,5,6,7,8] keys were used in the blocks with granularity levels of 2, 4, and 8, respectively. The participants were instructed to use a specific finger for pressing each key: the index, middle, ring, and little fingers were to be used for the [4,5], [3,6], [2,7], and [1,8] keys, respectively. The left hand was assigned to the [1,2,3,4] keys, and the right hand was assigned to the [5,6,7,8] keys.

Experiment 2

In Exp 2, the procedure was identical to that of Exp 1, except that beep sounds were used instead of ring stimuli. The beeps were classified based on pitch rather than size, with a specific pitch boundary set at 170 Hz. The beep sounds were created using a Psychtoolbox function called 'Beeper.m'. The volume of the sounds was adjusted individually to ensure that each participant could comfortably hear them throughout the entire experiment. The order of Exp 1 and 2 was randomized across participants: 26 and 32 of them performed Exp 1 and 2 first, respectively.

Experiment 3

In Exp 3, eighteen of the individuals who participated in Exp 1 and 2 took part. On each trial, participants performed either the ring size classification task (the one used in Exp 1) or the sound pitch classification task (the one used in Exp 2). The task was randomly chosen for each trial and was indicated at the start of the trial by displaying the words “Ring” or “Pitch” on the screen. The level of classification granularity alternated between 2 and 4 on a block-to-block basis. For each participant, the ring sizes and sound pitches were sampled from the same tailored distributions used in Exp 1 and 2, respectively.

To prevent any factors associated with motor or action space from confounding the transfer of granularity effect between visual and auditory modalities, we made participants use the fingers of the

different hands for the two tasks. In the blocks with the granularity level of 2, the [2,3] keys were pressed by the third and middle fingers, respectively, of the left hand for ring size classification while the [6,7] keys were pressed by the middle and third fingers, respectively, of the right hand for sound pitch classification (the row labeled by "$G = 2$" in Fig. 5b). In the blocks with the granularity level of 4, the [1,2,3,4] keys were pressed by the ring, third, middle, and index fingers, respectively, of the left hand for ring size classification while the [5,6,7,8] keys were pressed by the index, middle, third, and ring fingers, respectively, of the right hand for sound pitch classification (the row labeled by "$G = 4$" in Fig. 5b).

Experiment 4

In Exp 4, eighteen of the individuals who participated in Exp 1 and 2 took part. The procedure of Exp 4 was similar to that of Exp 1. Participants performed the ring size classification task, beginning with alternating blocks of the training and testing trials, followed by a period of testing-trial-only blocks. Exp 4 aimed to determine the temporal locus of the granularity effect, specifically whether the choice-attraction bias increases as a function of the granularity in the previous trial or the current trial. To investigate this, Exp 4 included two types of trial blocks: one with fixed granularity at the level of 2 and the other with varying granularity between two levels, 2 and 8. Comparing the trials between the two types of blocks allowed us to create two critical conditions: one in which the granularity varied in the previous trial but fixed in the current trial (marked by the orange dashed box and letters in Fig. 3), and the other in which the granularity fixed in the previous trial but varied in the current trial (marked by the green dashed box and letters in Fig. 3). Exp 4 began with the alternating training and testing blocks for the first 16 blocks, which were followed by the testing blocks for the remaining 20 blocks, each block consisting of 50 trials.

To address potential confounds related to cognitive load in switching action maps, we carefully assigned keys to choices in the following way. In the blocks with fixed granularity, we alternated key assignments between the [c,v] keys and the [4,5] keys (as shown in the bottom panels of Fig. 3). In the blocks with varying granularity, we alternated key assignments between using the [c,v] keys for the granularity level of 2 and the [1,2,3,4,5,6,7,8] keys for the granularity level of 8 (as shown in the top panels of Fig. 3). The fingers were assigned to the keys in the same way as in Exp 1, except that the left and right thumbs were assigned to the [c,v] keys.

Experiment 5

Exp 5 aims to determine if the granularity effect can be generalized across different perceptual tasks depending on whether the tasks require the same decision variable (DV). Three different tasks were performed on ring stimuli: (i) classification task, (ii) scaling task, and (iii) reproduction task. The overall procedure of the classification task was similar to that used in Exp 1, 3, and 4. In the scaling task, participants were shown a ring and asked to judge which quantile its size belongs to within the entire size distribution. They did this by moving a vertical line along a scale bar continuously within 3 s. Eleven ticks were evenly spaced over the scale bar to guide participants' estimation. Initially, the line appeared at a random position over the scale bar with equal probability. In the reproduction task, participants were required to adjust the diameter of a probe ring to match the absolute size of the target ring within 3 s. The physical appearance of the probe ring was identical to the target ring, except for the diameter. The probe ring's initial size was randomly sampled from the same distribution as the target ring.

In any given block of trials, two tasks were performed in succession as a pair over trials. Depending on which two of the three tasks were performed, there were two types of blocks (Fig. 4a). On

each trial of the 'classification-scaling' blocks, participants performed the classification task and then the scaling task. On each trial of the 'classification-reproduction' blocks, participants performed the classification task and then the reproduction task. For each block type, the granularity level varied between two granularity levels, 2 and 8, on a block-to-block basis. At the start of each trial, a pre-cue (0.5 s) indicated which keys should be used for reporting the class by presenting "45" for granularity level 2 or "12345678" for granularity level 8. Then, a ring stimulus was viewed for 1.5 s and classified by participants within 1.5 s after stimulus onset. After classification, a pre-cue for the scaling or reproduction task, "cv," appeared for 0.5 s, indicating which keys should be used for scaling and reproduction. Then, a new ring stimulus was viewed for 1.5 s, and participants carried out the scaling or reproduction tasks on that ring. In any given trial, the sizes of the ring for classification and that for scaling or reproduction were independently sampled from the same calibrated (see below) stimulus distribution.

Since any participants in Exp 5 did not take part in Exp 1, we ran the threshold-calibration blocks before administering the training and testing blocks. The threshold-calibration blocks followed the same procedure as Experiment 1, with the exception that the stimuli were solid purple rings (1.219 cd/m2), and two blocks, each consisting of 60 trials, were administered. In the training and testing blocks, we used the purple rings with the same appearance as those in the threshold-calibration blocks. The ring size was randomly sampled for each trial from the distribution calibrated by the threshold-calibration blocks, as in the previous experiments.

As similarly done in Exp 1, the threshold calibration blocks were initially followed by the alternating training and testing blocks for the first 16 blocks (2 blocks for each of the 8 conditions: [testing, training] x [granularity = 2,8] x [reproduction, scaling task]), and then solely by the testing blocks for the remaining 4 blocks (one block for each of the 4 conditions: [granularity = 2,8] x [reproduction, scaling task]). Each testing and training block consisted of 15 and 35 trials, respectively. As a result, a total of 105 testing trials (3 blocks x 35 trials) were acquired for each condition.

The training and testing blocks differed only in that trial-to-trial corrective feedback was provided only in the former. The feedback for the classification task was the same as that of Exp 1. For the scaling task, a green vertical line was presented for 0.5 s at the position corresponding to the true relative size over the scale bar. For the reproduction task, a green ring with the actual size of the target ring was presented for 0.5 s.

Experiment 6

The procedure for Exp 6 is the same as that of Exp 5, with the following exceptions: (i) stimuli were displayed for 0.3 seconds in both the training and testing blocks; (ii) the ticks were not shown on the scale bar in the scaling task to prevent participants from treating it as a discrete categorization task; (iii) a mask (consisting of white dots randomly distributed around the ring) lasting for 1 s followed the ring stimulus for the scaling and reproduction tasks to minimize aftereffects.

Experiment 7

In Exp 7, thirty of the individuals who participated in Exp 1 and 2 took part. Exp 7 was conducted to examine whether the granularity can be explained away by the correspondence in motor responses or action space between consecutive trials. The procedure of Exp 7 was the same as that of Exp 3, with the following exceptions. First, the ring size and sound pitch classification tasks were varied on a block-to-block basis. Second, during the pre-cue period, one of the characters, 'L' and 'R', randomly appeared on

each trial to indicate which side of the hands should be used to report. The [1,2,3,4] and [5,6,7,8] keys were assigned to the little, ring, middle, and index fingers of the left hand and he index, middle, ring, and little fingers of the hand, respectively. In the blocks with granularity level 2, [2,3] (or [6,7]) keys were used to report the 1st and the 2nd classes, respectively. In the blocks with granularity level 4, [1,2,3,4] (or [5,6,7,8]) keys were used to report from the 1st to 4th classes, respectively.

There were 36 blocks in total, each consisting of 50 trials. The classification granularity varied between 2 and 4. Exp 7 began with the alternating training and testing blocks for the first 16 blocks (4 blocks for each of the 4 conditions: [testing, training] x [granularity = 2,4]), which were followed by the testing blocks for the remaining 20 blocks (10 blocks for each of the 2 conditions: [granularity = 2,4]).

Assessing history effects

To comprehensively assess the history effects, including the granularity effect, on the current choice, we regressed the current choice c_t onto multiple factors: previous choices (c_{t-i}); interactions of previous choice with granularity ($c_{t-i} \times G$), with previous RT ($c_{t-i} \times RT_{t-i}$), and with current RT ($c_{t-i} \times RT_t$); previous stimuli (s_{t-i}); interaction of previous stimuli with granularity ($s_{t-i} \times G$), with previous RT ($s_{t-i} \times RT_{t-i}$), and with current RT ($s_{t-i} \times RT_t$); current stimulus (s_t); interactions of current stimulus with granularity ($s_t \times G$) and with current RT ($s_t \times RT_t$).
The following regression model was used for Exp 1 and 2:

$$c_t \sim \sum_{i=1}^{10} \big(\beta_{c_{t-i}} c_{t-i} + \beta_{c_{t-i}\times G} c_{t-i} \times G + \beta_{c_{t-i}\times RT_{t-i}} c_{t-i} \times RT_{t-i} + \beta_{c_{t-i}\times RT_t} c_{t-i} \times RT_t + \beta_{s_{t-i}} s_{t-i} + \beta_{s_{t-i}\times G} s_{t-i} \times G + \beta_{s_{t-i}\times RT_{t-i}} s_{t-i} \times RT_{t-i} + \beta_{s_{t-i}\times RT_t} s_{t-i} \times RT_t\big) + \beta_{s_t} s_t + \beta_{s_t\times G} s_t \times G + \beta_{s_t\times RT_t} s_t \times RT_t + \beta_0 \quad [Eq\ 1]$$

, where β_0 accounts for any arbitrary constant bias in choice selection. In this regression, the data from individual participants were concatenated to calculate the coefficients. The non-interaction regressors such as c_t, s_t, and RT_t were standardized to have a mean of 0 and a standard deviation of 1 for each block of trials. This block-wise standardization was done to prevent any potential block-to-block history effects from interfering with the trial-to-trial history effects, which are the main focus of this study. Consequently, the interaction regressors involving those standardized factors were the products of two standardized factors. The granularity levels, [2, 4, 8], were coded into G values, [0, 1, 2]. This allowed $\beta_{c_{t-i}}$ and $\beta_{s_{t-i}}$ to solely account for the history effects of the previous choice and stimulus, respectively, when the granularity level was 2 by setting the interaction regressor terms involving G to zero. The regression model included a total of 84 coefficients as the regressors involved previous choices and stimuli up to ten trials back ($i = [1,10]$).

The p-values of the coefficients were estimated using a nonparametric bootstrapping procedure due to potential deviations from a normal distribution for ordinal categories. The estimation of p-values involved the following steps. First, 10,000 bootstrap datasets ($B = 10{,}000$) were generated from the original dataset by sampling with replacement. Second, for each bootstrap dataset, the multiple regression model [Eq 1] was applied to estimate a corresponding set of the 84 coefficients, resulting in a distribution of 10,000 bootstrap estimates for each coefficient. Third, for each distribution of bootstrap coefficients, a p-value was calculated by doubling the proportion of the bootstrap coefficients that fall in the minority side of 0, as a two-tailed test was applied. In cases where no such minority coefficients existed, p-values

were reported as "$p < 10^{-4}$" in the main text, where $10^{-4} = 1/B$. Lastly, these p-values were adjusted to control for false discovery rate (FDR) in multiple hypotheses testing [141].
The total number of hypotheses tested was equal to the number of coefficients, which was 84 for Exp 1 and 2.

The regression model for Exp 3 and 7, where the two tasks alternated on a trial-to-trial basis, was the same as [Eq 1], except that the regressors involved previous choices and stimuli only up to one trial back ($i = 1$). As a result, FDR was controlled for a total of 12 hypotheses.

In Exp 4, the regression model was the same as that in Exp 3 and 7, with a few exceptions. The granularity level varied, on a trial-to-trial basis, between 2 and 8, coded into G values of 0 and 1, respectively. Hence, G had trial indices: G_{t-1} and G_t when evaluating the granularity effects of the previous and current choices, respectively. Accordingly, for the dataset arranged for evaluating the granularity effect of the previous choice ($\beta_{c_{t-1}\times G_{t-1}}$), the regression model was as follows:

$$c_t \sim \beta_{c_{t-1}} c_{t-1} + \beta_{c_{t-1}\times G_{t-1}} c_{t-1} \times G_{t-1} + \beta_{c_{t-1}\times RT_{t-1}} c_{t-1} \times RT_{t-1} + \beta_{c_{t-1}\times RT_t} c_{t-1} \times RT_t + \beta_{s_{t-1}} s_{t-1} + \beta_{s_{t-1}\times G_{t-1}} s_{t-1} \times G_{t-1} + \beta_{s_{t-1}\times RT_{t-1}} s_{t-1} \times RT_{t-1} + \beta_{s_{t-1}\times RT_t} s_{t-1} \times RT_t + \beta_{s_t} s_t + \beta_{s_t\times G_{t-1}} s_t \times G_{t-1} + \beta_{s_t\times RT_t} s_t \times RT_t + \beta_0. \quad [Eq\ 2]$$

For the dataset arranged for evaluating the granularity effect of the current choice ($\beta_{c_{t-1}\times G_t}$), the regression model was as follows:

$$c_t \sim \beta_{c_{t-1}} c_{t-1} + \beta_{c_{t-1}\times G_t} c_{t-1} \times G_t + \beta_{c_{t-1}\times RT_{t-1}} c_{t-1} \times RT_{t-1} + \beta_{c_{t-1}\times RT_t} c_{t-1} \times RT_t + \beta_{s_{t-1}} s_{t-1} + \beta_{s_{t-1}\times G_t} s_{t-1} \times G_t + \beta_{s_{t-1}\times RT_{t-1}} s_{t-1} \times RT_{t-1} + \beta_{s_{t-1}\times RT_t} s_{t-1} \times RT_t + \beta_{s_t} s_t + \beta_{s_t\times G_t} s_t \times G_t + \beta_{s_t\times RT_t} s_t \times RT_t + \beta_0. \quad [Eq\ 3]$$

For these regression models, FDR was controlled for a total of 12 hypotheses.

In Exp 5 and 6, the regression model was the same as [Eq 2], with the following exceptions. First, there were no regressors involving RT_t because the task performed in the current trial was scaling or reproduction, and the response latency of this type of task is to that of discrete classification. Second, c_t was a continuous value ranging from 0 and 1 for the classification-scaling trials and an unbounded continuous value for the classification-reproduction trials. FDR was controlled for a total of 9 hypotheses. To illustrate how $\beta_{c_{t-i}}$ was modulated by G and varied across individual participants, we conducted additional regression analyses for each level of granularity and for each participant using the following model:

$$c_t \sim \sum_{i=1}^{10} \left(\beta_{c_{t-i}} c_{t-i} + \beta_{s_{t-i}} s_{t-i}\right) + \beta_{s_t} s_t + \beta_0. \quad [Eq\ 4]$$

The results of these regression analyses are shown in Figure 1b,d.

Bayesian model for parallel belief propagation in stimulus and DV spaces.

We have developed a Bayesian model to offer a principled and unified account of the history effects observed across the classification, scaling, and reproduction tasks: the stimulus-repulsion bias, choice-attraction bias, and granularity effect (Fig. 6a). This model shares many general assumptions with other Bayesian decision-making models (Ma and Jazayeri, 2014), such that: (i) When a task is given, human individuals learn an internal (generative) model of the causal structure of relevant random variables involved in the task, which may or may not reflect the true structure; (ii) As the state of any of those

variables is observed or known, they propagate it over the internal model to probabilistically infer the state of the variable critical to the task; (iii) They form a DV and commit to a decision by applying a decision rule to the current state of the DV. In order to explain the history effects within the Bayesian framework, the model further assumes that humans continually update their probabilistic knowledge in their internal model (beliefs) based on their trial-to-trial task episodes (Fig. 6d). Specifically, the model assumes that two prior beliefs are updated in parallel, independently of each other, regarding the stimuli and DV, respectively. This assumption of "parallel belief updating in stimulus and DV spaces" prescribes that the stimulus-repulsion bias originates from updating the belief about the stimuli, while the choice-attraction bias and its modulation by decision granularity originate from updating the belief about the DV. The model's rationale is stated in the main text, while statistical details are provided below.

Internal model for stimulus inference. The internal model for the stimulus space (IM^s) consists of two components of probabilistic knowledge, one about the stochastic causality of external stimuli (s) on their sensory measurements (m^s; left panel of Fig. 6b) and the other about the distribution of external stimuli encountered during the task. They can be expressed by $p(m^s|s) = \mathcal{N}(s, \sigma_s)$ and $p(s) = \mathcal{N}(s_0, \sigma_{s_0})$, respectively, where $\mathcal{N}(\mu, \sigma)$ denotes the normal distribution with mean μ and standard deviation σ. Observers use the Bayes rule to form a posterior belief about the stimulus $p(s|m^s)$ when they sense the state of m^s is sensed in their sensory apparatus. This is done by propagating the sensed state of m^s over IM^s, which is proportional to $p(m^s|s)p(s)$ (left panel of Fig. 6c). As a point estimate of the stimulus $\hat{s}$ (left panel of Fig. 6c), observers take the mode of the posterior belief (maximum a posteriori) applying the L1 loss function $L = \sum|s_t - \hat{s}_t|$. Observers adjust the size of the probe ring to align with $\hat{s}$ in the reproduction task.

Internal model for DV inference. To perform the scaling and classification tasks, observers need to learn the internal model for the DV space (IM^{DV}). IM^{DV} also consists of two components of probabilistic knowledge, one about the stochastic causality of DV states (v) on their internal measurements (m^v; right panel of Fig. 6b) and the other about the distribution of DV states formed during the task. Since, v unlike s in IM^s, is bounded between 0 and 1, we defined the shapes of $p(m^v|v)$ and $p(v)$ by assuming that given a point value of v, its measurement m^v diffuses from v via Brownian motion while turning its direction at the bounds. We will denote the resultant distribution of the particles of this bounded Brownian motion by $B(v, \sigma_v)$, where v is the starting point of diffusion and σ_v is the strength of diffusion. $B(v, \sigma_v)$ is derived as follows. First, the particles are distributed in an effectively bounded space, $[-b, b]$, as a normal distribution, $\mathcal{N}(v, \sigma_v)$. The space is "effectively bounded" because we fixed b to 4 while the maximum value of σ_v we have considered in the following simulation was 0.2. Therefore, even if v and σ_v have their greatest values 1 and 0.2, respectively, $N(v, \sigma_v)$ is effectively 0 at the bound of the space because $N(b; v = 1, \sigma_v = 0.2)/N(v; v = 1, \sigma_v = 0.2) < 10^{-48}$. Then, $\mathcal{N}(v, \sigma_v)$ defined in $[-b, b]$ is truncated into $B(v, \sigma_v)$ defined in $[0, 1]$. In doing so, the part of $\mathcal{N}(v, \sigma_v)$ within $[-b, 0)$ is flipped to $[0, b]$ and added to the part of $\mathcal{N}(v, \sigma_v)$ within $[0, b]$. We will denote the distribution after this first round of truncation by $\mathcal{N}(v, \sigma_v)^1$. On the second round, the part of $\mathcal{N}(v, \sigma_v)^1$ within $(1, b]$ is flipped to $[-b + 1,1]$ and added to the part of $\mathcal{N}(v, \sigma_v)^1$ in $[-b + 1,1]$. The distribution after the second round is denoted as $\mathcal{N}(v, \sigma_v)^2$. This truncation procedure is repeated n times until the part of $\mathcal{N}(v, \sigma_v)^n$ falling outside of [0,1] is 0. We denote $\mathcal{N}(v, \sigma_v)^n$ as $B(v, \sigma_v)$. Thus, the likelihood of v given m^v is defined as $p(m^v|v) = B(m^v, \sigma_v)$. Then, when the state of m^v is known, a posterior belief about the DV can be formed by propagating the known state of m^v over IM^{DV}: $p(v|m^v) \propto p(m^v|v)p(v)$. The same

estimation rule (MAP based on the L1 loss function) is applied to obtain a point estimate of DV $\hat{v}$ from the posterior distribution. Observers adjust the location of the probe line to align with $\hat{v}$ on the scale bar in the scaling task. As for the classification task, observers apply the following decision rule: (i) they establish a set of criteria to evenly divide the DV space based on the decision granularity level ($[0.5]$ for 2; $[0.25, 0.5, 0.75]$ for 4; $[0.125, 0.25, \ldots, 0.75, 0.875]$ for 8); (ii) commit to a choice corresponding to a subregion of the DV space within which $\hat{v}$ falls.

Origin of DV measurements. We did not specify the origin of m^v (the evidence for v) when we described IM^{DV} above, to avoid complications. This specification is essential for connecting the two internal models, IM^s and IM^{DV}, and requires a separate description with a clear rationale and sufficient details. In both scaling and classification tasks, the true state of DV is, by definition, the probability that the current state of the stimulus s_t is larger than the entire possible states of s, which is equal to the cumulative distribution function of s for the interval from negative infinity to s_t: $v(s_t) = \int_{-\infty}^{s_t} p(s)ds$. However, $v(s_t)$ is not directly available since s_t cannot be observed but only inferred from its sensory evidence m_t^s. This means that not the true state of DV ($v(s_t)$) but only its "evidence" is available. By substituting s_t with $\hat{s}_t$, which is inferred from the sensory evidence with the prior knowledge of s in IM^s, we can define the evidence for v: $m^v = \int_{-\infty}^{\hat{s}} p(s)ds$ (angled arrow at the top of Fig. 6c). To sum in general terms, the outcome of the probabilistic inference based on a sensory measurement with $IM^s(\hat{s})$ is converted by the absolute-to-relative mapping function ($\Phi(s) = \int p(s)ds$; the middle panel of Fig. 6d) into the evidence for inferring the true state of DV with $IM^{DV}(m^v)$. Due to this conversion, the same stimulus estimate $\hat{s}$ can result in different states of m^v depending on the shape and location of the stimulus prior $p(s)$.

Belief updating in stimulus space. So far, we have defined the internal models for the stimulus and DV spaces and described how observers carry out the reproduction, scaling, and classification tasks based on the inferred outcomes with those internal models, $\hat{s}$ and $\hat{v}$. Next, we will specify how some beliefs in the two internal models are updated based on the events occurring over trial episodes. The prior beliefs about stimulus and DV distributions, $p(s)$ and $p(v)$, are updated in parallel. Let us denote the stimulus prior used to perform a task on the previous trial by $p(s)$, the memory of sensory measurement by mm_{t-1}^s, and the stimulus prior that is updated after the previous trial and will be used in the current trial by $p(s)'$. Then the stimulus prior should be updated toward mm_{t-1}^s since mm_{t-1}^s provides new evidence for the stimulus distribution. This updating process is captured by formalizing the prior of s in the current trial as the posterior of s in the previous trial, as follows: $p(s_t)' = p(s|mm_{t-1}^s) \propto p(mm_{t-1}^s|s)p(s)$ (the left panel of Fig. 6d). Here, since mm_{t-1}^s is assumed to be subject to unbiased diffusion error over time in memory, mm_{t-1}^s is randomly sampled in each trial from $\mathcal{N}(s_t, \sigma_{s'})$, where s_t is the stimulus at trial t and $\sigma_{s'}^2$ is the sum of sensory and memory variance, $\sigma_{s'}^2 \equiv \sigma_s^2 + \sigma_{mm^s}^2$. Thus, the likelihood of s given mm_{t-1}^s is defined as $\mathcal{N}(mm_{t-1}^s, \sigma_{s'})$.

Belief updating in DV space. The belief updating process in DV space shares the basic rationale with that in stimulus space: the prior belief about v is continually updated over trials. However, whereas the prior belief about s is updated by mm^s, the prior belief about v is updated by decision commitment. Specifically, the state space of v is reduced to a subregion corresponding to the states of v consistent with the choice. In other words, the prior of v for the current trial $p(v_t)'$ is the probability distribution of v conditioned on the previous choice, as follows: $p(v_t)' = p(v|choice_{t-1}) \propto p(choice_{t-1}|v)p(v)$ (the right panel of Fig. 6d). An important implication of this conditioning is that as the decision becomes more

granular, the state space of v is further reduced. Additionally, the conditioned prior has a memory leak so that the prior can have values greater than 0 outside the range (Fig. 1b). This leak on the DV prior was implemented by convoluting it with a normal distribution, $\mathcal{N}(0, \sigma_{leak})$. To bound the convolved prior belief within $[0, 1]$, the aforementioned truncation procedure is also applied.

In sum, our Bayesian model account of the history effects in the reproduction, scaling, and classification tasks is defined by the two internal models for inferring the stimulus and DV states (IM^s and IM^{DV}) and the algorithms of belief updating of the prior beliefs in those two internal models, which are fully specified by a total of six free parameters, $[s_0, \sigma_{s_0}, \sigma_s, \sigma_{mm^s}, \sigma_v, \sigma_{leak}]$.

Alternative models for the granularity effect

Considering the necessity of updating beliefs in DV space for the granularity effect, we explored previously suggested sources of history effects as potential alternative explanations for the granularity effect identified in our study. To this end, we built three alternative models that implement those suggestions by modifying the original Bayesian model described in the previous section. We emphasize that all of these alternative models share a common feature: none of them assume probabilistic inference or belief updating in DV space. Below, the original Bayesian model will be referred to as 'the standard model.'

Sensory adaptation model. The sensory adaptation model assumes that the response gain of sensory neurons encoding the stimulus in the previous trial is reduced. This model is identical to the standard model except for the following. First, the response gain of the sensory neurons tuned to the stimulus measurement in the previous trial m_{t-1}^s is selectively suppressed, which is incorporated in the model by reducing the gain of likelihood function around m_{t-1}^s. Specifically, the suppressed gain, $f_s(x)$, is described by $f_s(x) = 1 - g\mathcal{N}(x; m_{t-1}^s, \sigma_s)$, where g is the parameter that modulates the strength of gain reduction. Consequently, for a given present stimulus measurement, the likelihood function is modified to $p(m_t^s|s) = f_s(x)N(x; m_t^s, \sigma_s)$. Second, it does not involve any process of belief updating in stimulus space. Third, since there is no informative prior in the DV space, the DV estimate $\hat{v}$ is the same as the DV measurement m^v. Four parameters, $[s_0, \sigma_{s_0}, \sigma_s, g]$, specify the model.

Stimulus-prior-updating-by-the-stimulus model. The stimulus-prior-updating-by-the-stimulus model is identical to the standard model except that it does not involve any process of probabilistic inference in the DV space. The model shares the same internal model for stimulus inference and the same belief updating in stimulus space as the standard model. Thus, it performs the reproduction task in exactly the same way as the standard model. On the other hand, the model carries out the scaling and classification task using the uninformative DV prior, similar to the sensory adaptation model. However, note that this model does not assume any sensory gain reduction at all, unlike the sensory adaptation model. Four parameters, $[s_0, \sigma_{s_0}, \sigma_s, \sigma_{mm^s}]$, specify the model.

Stimulus-prior-updating-by-the-choice model. Like the stimulus-prior-updating-by-the-stimulus model, the stimulus-prior-updating-by-the-choice model shares the same internal model for stimulus inference as the standard model. However, this model differs from the stimulus-prior-updating-by-the-stimulus model in that it updates its stimulus prior not only based on the memory of the previous memory mm_{t-1}^s but also based on decision commitment. Specifically, the updated stimulus prior, $p(s)'$, is updated to be

	Sensory adaptation model	Stimulus-prior-updating-by-the-choice model	Stimulus-prior-updating-by-the-choice model	Standard model
σ_{s_0}	$[0.4, 4]$	$[0.4, 4]$	$[0.4, 4]$	$[0.4, 4]$
σ_s	$[0.1, 1]$	$[0.1, 1]$	$[0.1, 1]$	$[0.1, 1]$
g	$[0.1, 1]$	-	-	-
σ_{mm^s}	-	$[0.4, 4]$	$[0.4, 4]$	$[0.4, 4]$
σ_{leak}	-	-	$[0.2, 2]$	$[0.02, 0.2]$
σ_v	-	-	-	$[0.02, 0.2]$

Table 1 | The range of parameters used in model simulation. For each parameter, 10 values were selected for the model simulation, evenly spaced within the given parameter range. For example, if the range is $[1, 10]$, the parameter values tested are the integers from 1 to 10.

consistent with the previous choice, c_{t-1}, as $p(v)'$ is updated to be consistent with the previous choice in the standard model. Thus, this model implements the possibility that the granularity might arise in stimulus space instead of DV space. For example, when the level of granularity was 4 and the previous stimulus was classified as the third class, observers consider that the previous stimulus was sampled within the range that is consistent with the third class. This consideration narrows down the stimulus prior to the range corresponding to the third class, which can be calculated based on the stimulus prior to be $[\Phi(0.5), \Phi(0.75)]$, where Φ is the inverse cumulative distribution of the updated prior, $p(s)'$. Then, the prior value outside the range is 0. This conditioned prior, $p(s)''$, is defined as $p(s)'' \propto p(s)'$, where s is within $[\Phi(0.5), \Phi(0.75)]$. Otherwise, $p(s)'' = 0$. Also, it is assumed that the conditioned prior has a leak so that the prior can have values greater than 0 outside the range. This leak is implemented by convoluting a normal distribution, $N(0, \sigma_{leak})$, with the conditioned prior, $p(s)''$. Thus, the model has five parameters, $[s_0, \sigma_{s_0}, \sigma_s, \sigma_{mm^s}, \sigma_{leak}]$.

Model simulation

To determine if the models can qualitatively display the history effects seen in our study's human participants, we conducted simulations using the following procedure. First, we randomly sampled 1,000 stimulus magnitudes from a normal distribution, $\mathcal{N}(0,1)$. Then, we let the models perform the reproduction, scaling, and classification tasks on this same sequence of stimuli while varying their model parameters. Over these trials, decision granularities were randomly varied trial-to-trial between 2 and 8. Then, the sequence of responds made by the models was regressed onto the regressors involving the stimulus and choice factors, using the following regression model:

$$y_t \sim \beta_{c_{t-1}} c_{t-1} + \beta_{c_{t-1} \times G_{t-1}} c_{t-1} \times G_{t-1} + \beta_{s_{t-1}} s_{t-1} + \beta_{s_{t-1} \times G_{t-1}} s_{t-1} \times G_{t-1} + \beta_{s_t} s_t + \beta_{s_t \times G_{t-1}} s_t \times G_{t-1} + \beta_0 , \quad [Eq\ 3]$$

where c_t, s_t, and G_t are classification choice, stimulus, and granularity levels at the trial t, and y_t was varied for each task. The response time was not included as a regressor because the models did not produce response times. To be consistent with the human experiments, we included the trials in which the level of granularity in the current trial was 2. The entire procedure outlined above was repeated 100 times

for each set of parameters, with a newly sampled sequence of 1000 stimulus magnitudes for each repetition. Then, the regression coefficients acquired from these 100 repetitions were averaged.

The model parameters used in the above simulations were determined as follows. In order to thoroughly and impartially explore the parameter space, we used all combinations of parameters selected from 10 evenly spaced parameter values. The specified range of the parameter space can be found in Table 1. For simplicity, we set the mean of the stimulus prior, s_0, as 0 for all models because the overall prior bias would not induce systematic bias to history effects. As a result, there were 10^3 parameter sets for the sensory adaptation and stimulus-prior-updating-by-the-stimulus models, 10^4 for the stimulus-prior-updating-by-the-choice model, and 10^5 for the standard (original Bayesian) model.

From these simulation results, we selected the best simulation parameter set as the one with the smallest sum of errors in the regression coefficients compared to human participants. For each task, the regression model $[Eq\ 3]$ consisted of 7 coefficients. Consequently, for the three tasks combined, there were 21 coefficients. The bias terms were excluded from the error calculation as our focus is on history effects. Likewise, β_{s_t} and $\beta_{s_t \times G_{t-1}}$ of the reproduction and scaling tasks were also excluded from the error calculation. This exclusion was based on the understanding that β_{s_t} reflects the task performance and that the task performance would be significantly affected by motor noise on the reproduction and scaling tasks for human participants, unlike the classification task which is not part of the current modeling. Thus, the error was the sum of the absolute errors of the 14 coefficients, excluding 3 coefficients related to the bias terms and 4 coefficients related to s_t (i.e., β_{s_t} and $\beta_{s_t \times G_{t-1}}$) on the scaling and reproduction tasks from the error calculation of the 21 coefficients.

Acknowledgments

This research was supported by the National Research Foundation of Korea funded by the Ministry of Science and ICT (RS-2024-00435727, RS-2024-00349515, RS-2023-00276729)

Data and code availability

Data and code will be available after publication.

References

1 Green, D. M. & Swets, J. A. *Signal detection theory and psychophysics*. Vol. 1 (Wiley New York, 1966).
2 Padoa-Schioppa, C. Neurobiology of economic choice: a good-based model. *Annual review of neuroscience* **34**, 333-359 (2011).
3 Wald, A. & Wolfowitz, J. Optimum character of the sequential probability ratio test. *The Annals of Mathematical Statistics*, 326-339 (1948).
4 Good, I. J. Studies in the history of probability and statistics. XXXVII AM Turing's statistical work in World War II. *Biometrika*, 393-396 (1979).
5 Arnauld, A. & Nichole, P. The art of thinking: Port-Royal logic (Dickoff J, James P, translators). *Indianapolis: Bobbs-Merrill* (1982).

6 Asanuma, H. & Sakata, H. Functional organization of a cortical efferent system examined with focal depth stimulation in cats. *Journal of Neurophysiology* **30**, 35-54 (1967).
7 Pavlov, P. I. Conditioned reflexes: an investigation of the physiological activity of the cerebral cortex. *Annals of neurosciences* **17**, 136 (2010).
8 Penfield, W. *The mystery of the mind: A critical study of consciousness and the human brain*. (Princeton University Press, 2015).
9 Gold, J. I. & Shadlen, M. N. The neural basis of decision making. *Annu. Rev. Neurosci.* **30**, 535-574 (2007).
10 Ma, W. J. & Jazayeri, M. Neural coding of uncertainty and probability. *Annual review of neuroscience* **37**, 205-220 (2014).
11 Kriegeskorte, N. & Diedrichsen, J. Peeling the onion of brain representations. *Annual review of neuroscience* **42**, 407-432 (2019).
12 Sternberg, R. J. Adaptive intelligence: Intelligence is not a personal trait but rather a person× task× situation interaction. *Journal of Intelligence* **9**, 58 (2021).
13 Craik, K. J. W. *The nature of explanation*. Vol. 445 (CUP Archive, 1967).
14 Platt, M. L. & Glimcher, P. W. Neural correlates of decision variables in parietal cortex. *Nature* **400**, 233-238 (1999).
15 Luce, P. A. A computational analysis of uniqueness points in auditory word recognition. *Perception & Psychophysics* **39**, 155-158 (1986).
16 Roitman, J. D. & Shadlen, M. N. Response of neurons in the lateral intraparietal area during a combined visual discrimination reaction time task. *Journal of neuroscience* **22**, 9475-9489 (2002).
17 Ratcliff, R. & Smith, P. L. A comparison of sequential sampling models for two-choice reaction time. *Psychological review* **111**, 333 (2004).
18 Romo, R., Hernández, A. & Zainos, A. Neuronal correlates of a perceptual decision in ventral premotor cortex. *Neuron* **41**, 165-173 (2004).
19 Lo, C.-C. & Wang, X.-J. Cortico–basal ganglia circuit mechanism for a decision threshold in reaction time tasks. *Nature neuroscience* **9**, 956-963 (2006).
20 Hanks, T. D., Ditterich, J. & Shadlen, M. N. Microstimulation of macaque area LIP affects decision-making in a motion discrimination task. *Nature neuroscience* **9**, 682-689 (2006).
21 Rangel, A., Camerer, C. & Montague, P. R. A framework for studying the neurobiology of value-based decision making. *Nature reviews neuroscience* **9**, 545-556 (2008).
22 Vlaev, I., Chater, N., Stewart, N. & Brown, G. D. Does the brain calculate value? *Trends in cognitive sciences* **15**, 546-554 (2011).
23 Kelly, S. P. & O'Connell, R. G. Internal and external influences on the rate of sensory evidence accumulation in the human brain. *Journal of Neuroscience* **33**, 19434-19441 (2013).
24 Latimer, K. W., Yates, J. L., Meister, M. L., Huk, A. C. & Pillow, J. W. Single-trial spike trains in parietal cortex reveal discrete steps during decision-making. *Science* **349**, 184-187 (2015).
25 Tsetsos, K. *et al.* Economic irrationality is optimal during noisy decision making. *Proceedings of the National Academy of Sciences* **113**, 3102-3107 (2016).
26 Brosnan, M. B. *et al.* Evidence accumulation during perceptual decisions in humans varies as a function of dorsal frontoparietal organization. *Nature Human Behaviour* **4**, 844-855 (2020).
27 Brunton, B. W., Botvinick, M. M. & Brody, C. D. Rats and humans can optimally accumulate evidence for decision-making. *Science* **340**, 95-98 (2013).
28 Drugowitsch, J., Wyart, V., Devauchelle, A.-D. & Koechlin, E. Computational precision of mental inference as critical source of human choice suboptimality. *Neuron* **92**, 1398-1411 (2016).
29 Waskom, M. L. & Kiani, R. Decision making through integration of sensory evidence at prolonged timescales. *Current Biology* **28**, 3850-3856. e3859 (2018).
30 Palmer, J., Huk, A. C. & Shadlen, M. N. The effect of stimulus strength on the speed and accuracy of a perceptual decision. *Journal of vision* **5**, 1-1 (2005).

31 Huk, A. C. & Shadlen, M. N. Neural activity in macaque parietal cortex reflects temporal integration of visual motion signals during perceptual decision making. *Journal of Neuroscience* **25**, 10420-10436 (2005).
32 Heitz, R. P. & Schall, J. D. Neural mechanisms of speed-accuracy tradeoff. *Neuron* **76**, 616-628 (2012).
33 Hanks, T., Kiani, R. & Shadlen, M. N. A neural mechanism of speed-accuracy tradeoff in macaque area LIP. *Elife* **3**, e02260 (2014).
34 Gabriel, M. *The meaning of thought*. (John Wiley & Sons, 2020).
35 Gershman, S. J., Horvitz, E. J. & Tenenbaum, J. B. Computational rationality: A converging paradigm for intelligence in brains, minds, and machines. *Science* **349**, 273-278 (2015).
36 Meyniel, F., Sigman, M. & Mainen, Z. F. Confidence as Bayesian probability: From neural origins to behavior. *Neuron* **88**, 78-92 (2015).
37 Pouget, A., Drugowitsch, J. & Kepecs, A. Confidence and certainty: distinct probabilistic quantities for different goals. *Nature neuroscience* **19**, 366-374 (2016).
38 Dong, D. W. & Atick, J. J. Statistics of natural time-varying images. *Network: computation in neural systems* **6**, 345 (1995).
39 Pearl, J. Models, reasoning and inference. *Cambridge, UK: CambridgeUniversityPress* **19**, 3 (2000).
40 Puga, J. L., Krzywinski, M. & Altman, N. Points of significance: Bayesian statistics. *Nature Methods* **12** (2015).
41 Cicchini, G. M., Mikellidou, K. & Burr, D. C. The functional role of serial dependence. *Proceedings of the Royal Society B* **285**, 20181722 (2018).
42 Akaishi, R., Umeda, K., Nagase, A. & Sakai, K. Autonomous mechanism of internal choice estimate underlies decision inertia. *Neuron* **81**, 195-206 (2014).
43 Fritsche, M., Spaak, E. & De Lange, F. P. A Bayesian and efficient observer model explains concurrent attractive and repulsive history biases in visual perception. *Elife* **9**, e55389 (2020).
44 Van Bergen, R. S. & Jehee, J. F. Probabilistic representation in human visual cortex reflects uncertainty in serial decisions. *Journal of Neuroscience* **39**, 8164-8176 (2019).
45 Treisman, M. & Williams, T. C. A theory of criterion setting with an application to sequential dependencies. *Psychological review* **91**, 68 (1984).
46 Lee, H., Lee, H.-J., Choe, K. W. & Lee, S.-H. Neural evidence for boundary updating as the source of the repulsive bias in classification. *Journal of Neuroscience* **43**, 4664-4683 (2023).
47 Lim, J. & Lee, S.-H. Spatial correspondence in relative space regulates serial dependence. *Scientific Reports* **13**, 18162 (2023).
48 Gold, J. I. & Stocker, A. A. Visual decision-making in an uncertain and dynamic world. *Annual Review of Vision Science* **3**, 227-250 (2017).
49 Lee, H. & Lee, S.-H. Boundary updating as a source of history effect on decision uncertainty. *Iscience* **26** (2023).
50 Lee, H.-J., Lee, H., Lim, C. Y., Rhim, I. & Lee, S.-H. Corrective feedback guides human perceptual decision-making by informing about the world state rather than rewarding its choice. *PLoS biology* **21**, e3002373 (2023).
51 Choe, K. W., Blake, R. & Lee, S.-H. Dissociation between neural signatures of stimulus and choice in population activity of human V1 during perceptual decision-making. *Journal of Neuroscience* **34**, 2725-2743 (2014).
52 Sheahan, H., Luyckx, F., Nelli, S., Teupe, C. & Summerfield, C. Neural state space alignment for magnitude generalization in humans and recurrent networks. *Neuron* **109**, 1214-1226. e1218 (2021).
53 Hachen, I., Reinartz, S., Brasselet, R., Stroligo, A. & Diamond, M. Dynamics of history-dependent perceptual judgment. *Nature communications* **12**, 6036 (2021).
54 Moon, J. & Kwon, O.-S. Attractive and repulsive effects of sensory history concurrently shape visual perception. *BMC biology* **20**, 247 (2022).

55 Bosch, E., Fritsche, M., Ehinger, B. V. & de Lange, F. P. Opposite effects of choice history and evidence history resolve a paradox of sequential choice bias. *Journal of vision* **20**, 9-9 (2020).
56 Urai, A. E., Braun, A. & Donner, T. H. Pupil-linked arousal is driven by decision uncertainty and alters serial choice bias. *Nature communications* **8**, 14637 (2017).
57 Urai, A. E., De Gee, J. W., Tsetsos, K. & Donner, T. H. Choice history biases subsequent evidence accumulation. *Elife* **8**, e46331 (2019).
58 Braun, A., Urai, A. E. & Donner, T. H. Adaptive history biases result from confidence-weighted accumulation of past choices. *Journal of Neuroscience* **38**, 2418-2429 (2018).
59 Kanervisto, A., Scheller, C. & Hautamäki, V. in *2020 IEEE conference on games (CoG).* 479-486 (IEEE).
60 Shaki, S. & Fischer, M. H. Deconstructing spatial-numerical associations. *Cognition* **175**, 109-113 (2018).
61 Loetscher, T., Schwarz, U., Schubiger, M. & Brugger, P. Head turns bias the brain's internal random generator. *Current Biology* **18**, R60-R62 (2008).
62 Hartmann, M., Grabherr, L. & Mast, F. W. Moving along the mental number line: Interactions between whole-body motion and numerical cognition. *Journal of Experimental Psychology: Human Perception and Performance* **38**, 1416 (2012).
63 Dehaene, S., Bossini, S. & Giraux, P. The mental representation of parity and number magnitude. *Journal of experimental psychology: General* **122**, 371 (1993).
64 Kersten, D., Mamassian, P. & Yuille, A. Object perception as Bayesian inference. *Annu. Rev. Psychol.* **55**, 271-304 (2004).
65 L Griffiths, T., Kemp, C. & B Tenenbaum, J. Bayesian models of cognition. (2008).
66 Ma, W. J. Bayesian decision models: A primer. *Neuron* **104**, 164-175 (2019).
67 Petzschner, F. H., Glasauer, S. & Stephan, K. E. A Bayesian perspective on magnitude estimation. *Trends in cognitive sciences* **19**, 285-293 (2015).
68 Palminteri, S., Wyart, V. & Koechlin, E. The importance of falsification in computational cognitive modeling. *Trends in cognitive sciences* **21**, 425-433 (2017).
69 Pascucci, D. *et al.* Laws of concatenated perception: Vision goes for novelty, decisions for perseverance. *PLoS biology* **17**, e3000144 (2019).
70 Gibson, J. J. Adaptation, after-effect, and contrast in the perception of tilted lines. II. Simultaneous contrast and the areal restriction of the after-effect. *Journal of Experimental Psychology* **20**, 553 (1937).
71 Stocker, A. A. & Simoncelli, E. Sensory adaptation within a Bayesian framework for perception. *Advances in neural information processing systems* **18** (2005).
72 Luu, L. & Stocker, A. A. Post-decision biases reveal a self-consistency principle in perceptual inference. *Elife* **7**, e33334 (2018).
73 Stocker, A. A. & Simoncelli, E. A Bayesian model of conditioned perception. *Advances in neural information processing systems* **20** (2007).
74 Summerfield, C. *Natural General Intelligence: How understanding the brain can help us build AI*. (Oxford University Press, 2022).
75 Tenenbaum, J. B., Kemp, C., Griffiths, T. L. & Goodman, N. D. How to grow a mind: Statistics, structure, and abstraction. *science* **331**, 1279-1285 (2011).
76 Romo, R., Hernández, A., Zainos, A., Lemus, L. & Brody, C. D. Neuronal correlates of decision-making in secondary somatosensory cortex. *Nature neuroscience* **5**, 1217-1225 (2002).
77 Heekeren, H. R., Marrett, S., Bandettini, P. A. & Ungerleider, L. G. A general mechanism for perceptual decision-making in the human brain. *Nature* **431**, 859-862 (2004). https://doi.org:10.1038/nature02966
78 Hebart, M. N., Schriever, Y., Donner, T. H. & Haynes, J.-D. The Relationship between Perceptual Decision Variables and Confidence in the Human Brain. *Cerebral Cortex* **26**, 118-130 (2014). https://doi.org:10.1093/cercor/bhu181

79 Xie, T. *et al.* Graded decisions in the human brain. *Nature Communications* **15**, 4308 (2024). https://doi.org:10.1038/s41467-024-48342-w
80 Gold, J. I. & Shadlen, M. N. Representation of a perceptual decision in developing oculomotor commands. *Nature* **404**, 390-394 (2000). https://doi.org:10.1038/35006062
81 Gold, J. I. & Shadlen, M. N. The influence of behavioral context on the representation of a perceptual decision in developing oculomotor commands. *J Neurosci* **23**, 632-651 (2003). https://doi.org:10.1523/jneurosci.23-02-00632.2003
82 Cisek, P. & Kalaska, J. F. Neural Correlates of Reaching Decisions in Dorsal Premotor Cortex: Specification of Multiple Direction Choices and Final Selection of Action. *Neuron* **45**, 801-814 (2005). https://doi.org:10.1016/j.neuron.2005.01.027
83 Shadlen, M. N., Hanks, T. D., Churchland, A. K., Kiani, R. & Yang, T. The speed and accuracy of a simple perceptual decision: a mathematical primer. (2006).
84 Huk, A. C. & Meister, M. L. Neural correlates and neural computations in posterior parietal cortex during perceptual decision-making. *Frontiers in integrative neuroscience* **6**, 86 (2012).
85 Hanks, T. D. & Summerfield, C. Perceptual Decision Making in Rodents, Monkeys, and Humans. *Neuron* **93**, 15-31 (2017). https://doi.org:10.1016/j.neuron.2016.12.003
86 Kool, W. & Botvinick, M. Mental labour. *Nature Human Behaviour* **2**, 899-908 (2018). https://doi.org:10.1038/s41562-018-0401-9
87 Taylor, M. & Creelman, C. D. PEST: Efficient estimates on probability functions. *The Journal of the Acoustical Society of America* **41**, 782-787 (1967).
88 Freedman, D. J. & Assad, J. A. Experience-dependent representation of visual categories in parietal cortex. *Nature* **443**, 85-88 (2006). https://doi.org:10.1038/nature05078
89 Law, C.-T. & Gold, J. I. Neural correlates of perceptual learning in a sensory-motor, but not a sensory, cortical area. *Nature Neuroscience* **11**, 505-513 (2008). https://doi.org:10.1038/nn2070
90 Fitzgerald, J. K., Freedman, D. J. & Assad, J. A. Generalized associative representations in parietal cortex. *Nature Neuroscience* **14**, 1075-1079 (2011). https://doi.org:10.1038/nn.2878
91 Mante, V., Sussillo, D., Shenoy, K. V. & Newsome, W. T. Context-dependent computation by recurrent dynamics in prefrontal cortex. *Nature* **503**, 78-84 (2013). https://doi.org:10.1038/nature12742
92 Lennie, P. The Cost of Cortical Computation. *Current Biology* **13**, 493-497 (2003). https://doi.org:10.1016/S0960-9822(03)00135-0
93 Levy, W. B. & Calvert, V. G. Communication consumes 35 times more energy than computation in the human cortex, but both costs are needed to predict synapse number. *Proceedings of the National Academy of Sciences* **118**, e2008173118 (2021).
94 Griffiths, T. L., Lieder, F. & Goodman, N. D. Rational Use of Cognitive Resources: Levels of Analysis Between the Computational and the Algorithmic. *Topics in Cognitive Science* **7**, 217-229 (2015). https://doi.org:https://doi.org/10.1111/tops.12142
95 Kiani, R. & Shadlen, M. N. Representation of Confidence Associated with a Decision by Neurons in the Parietal Cortex. *Science* **324**, 759-764 (2009). https://doi.org:doi:10.1126/science.1169405
96 Howes, A., Lewis, R. L. & Vera, A. Rational adaptation under task and processing constraints: implications for testing theories of cognition and action. *Psychological review* **116**, 717 (2009).
97 Icard, T. in *Proceedings of the Annual Meeting of the Cognitive Science Society.*
98 Lewis, R. L., Howes, A. & Singh, S. Computational rationality: Linking mechanism and behavior through bounded utility maximization. *Topics in cognitive science* **6**, 279-311 (2014).
99 Blackwell, D. A. & Girshick, M. A. *Theory of games and statistical decisions*. (Courier Corporation, 1979).
100 Laplace, P. S. *Théorie analytique des probabilités*. (Courcier, 1820).
101 Ferguson, T. S. *Mathematical statistics: A decision theoretic approach*. Vol. 1 (Academic press, 2014).
102 Berger, J. O. *Statistical decision theory and Bayesian analysis*. (Springer Science & Business Media, 2013).

103 Sohn, H. & Lee, S.-H. Dichotomy in perceptual learning of interval timing: calibration of mean accuracy and precision differ in specificity and time course. *Journal of neurophysiology* **109**, 344-362 (2013).
104 Körding, K. P. & Wolpert, D. M. Bayesian integration in sensorimotor learning. *Nature* **427**, 244-247 (2004).
105 Girshick, A. R., Landy, M. S. & Simoncelli, E. P. Cardinal rules: visual orientation perception reflects knowledge of environmental statistics. *Nature neuroscience* **14**, 926-932 (2011).
106 Jazayeri, M. & Shadlen, M. N. Temporal context calibrates interval timing. *Nature neuroscience* **13**, 1020-1026 (2010).
107 Tassinari, H., Hudson, T. E. & Landy, M. S. Combining priors and noisy visual cues in a rapid pointing task. *Journal of Neuroscience* **26**, 10154-10163 (2006).
108 Wei, X.-X. & Stocker, A. A. A Bayesian observer model constrained by efficient coding can explain'anti-Bayesian'percepts. *Nature neuroscience* **18**, 1509-1517 (2015).
109 Hahn, M. & Wei, X.-X. A unifying theory explains seemingly contradictory biases in perceptual estimation. *Nature Neuroscience* **27**, 793-804 (2024).
110 Bogacz, R., Brown, E., Moehlis, J., Holmes, P. & Cohen, J. D. The physics of optimal decision making: a formal analysis of models of performance in two-alternative forced-choice tasks. *Psychological review* **113**, 700 (2006).
111 Ratcliff, R. & McKoon, G. The diffusion decision model: theory and data for two-choice decision tasks. *Neural computation* **20**, 873-922 (2008).
112 Van Bergen, R. S., Ji Ma, W., Pratte, M. S. & Jehee, J. F. Sensory uncertainty decoded from visual cortex predicts behavior. *Nature neuroscience* **18**, 1728-1730 (2015).
113 Walker, E. Y., Cotton, R. J., Ma, W. J. & Tolias, A. S. A neural basis of probabilistic computation in visual cortex. *Nature Neuroscience* **23**, 122-129 (2020).
114 Pascucci, D. *et al.* Serial dependence in visual perception: A review. *Journal of Vision* **23**, 9-9 (2023).
115 Manassi, M., Murai, Y. & Whitney, D. Serial dependence in visual perception: A meta-analysis and review. *Journal of vision* **23**, 18-18 (2023).
116 Sheehan, T. C. & Serences, J. T. Attractive serial dependence overcomes repulsive neuronal adaptation. *PLoS biology* **20**, e3001711 (2022).
117 Barbosa, J. *et al.* Interplay between persistent activity and activity-silent dynamics in the prefrontal cortex underlies serial biases in working memory. *Nature neuroscience* **23**, 1016-1024 (2020).
118 John-Saaltink, E. S., Kok, P., Lau, H. C. & De Lange, F. P. Serial dependence in perceptual decisions is reflected in activity patterns in primary visual cortex. *Journal of Neuroscience* **36**, 6186-6192 (2016).
119 Sadil, P., Cowell, R. A. & Huber, D. E. The push–pull of serial dependence effects: Attraction to the prior response and repulsion from the prior stimulus. *Psychonomic Bulletin & Review* **31**, 259-273 (2024).
120 Manassi, M., Kristjánsson, Á. & Whitney, D. Serial dependence in a simulated clinical visual search task. *Scientific reports* **9**, 19937 (2019).
121 Fritsche, M., Mostert, P. & de Lange, F. P. Opposite effects of recent history on perception and decision. *Current Biology* **27**, 590-595 (2017).
122 Cicchini, G. M., Mikellidou, K. & Burr, D. Serial dependencies act directly on perception. *Journal of vision* **17**, 6-6 (2017).
123 Ceylan, G., Herzog, M. H. & Pascucci, D. Serial dependence does not originate from low-level visual processing. *Cognition* **212**, 104709 (2021).
124 Manassi, M., Liberman, A., Kosovicheva, A., Zhang, K. & Whitney, D. Serial dependence in position occurs at the time of perception. *Psychonomic bulletin & review* **25**, 2245-2253 (2018).
125 Gallagher, G. K. & Benton, C. P. Stimulus uncertainty predicts serial dependence in orientation judgements. *Journal of Vision* **22**, 6-6 (2022).

126 Sanders, J. I., Hangya, B. & Kepecs, A. Signatures of a statistical computation in the human sense of confidence. *Neuron* **90**, 499-506 (2016).
127 Suárez-Pinilla, M., Seth, A. K. & Roseboom, W. Serial dependence in the perception of visual variance. *Journal of vision* **18**, 4-4 (2018).
128 Samaha, J., Switzky, M. & Postle, B. R. Confidence boosts serial dependence in orientation estimation. *Journal of Vision* **19**, 25-25 (2019).
129 Fischer, J. & Whitney, D. Serial dependence in visual perception. *Nature neuroscience* **17**, 738-743 (2014).
130 Fritsche, M. & de Lange, F. P. The role of feature-based attention in visual serial dependence. *Journal of Vision* **19**, 21-21 (2019).
131 Pascucci, D. & Plomp, G. Serial dependence and representational momentum in single-trial perceptual decisions. *Scientific Reports* **11**, 9910 (2021).
132 Garner, W. R. An informational analysis of absolute judgments of loudness. *Journal of experimental psychology* **46**, 373 (1953).
133 Mori, S. & Ward, L. M. Pure feedback effects in absolute identification. *Perception & Psychophysics* **57**, 1065-1079 (1995).
134 Mori, S. Effects of stimulus information and number of stimuli on sequential dependencies in absolute identification. *Canadian Journal of Experimental Psychology/Revue canadienne de psychologie expérimentale* **52**, 72 (1998).
135 Stewart, N., Brown, G. D. & Chater, N. Absolute identification by relative judgment. *Psychological review* **112**, 881 (2005).
136 Griffiths, T. L., Chater, N., Norris, D. & Pouget, A. How the Bayesians got their beliefs (and what those beliefs actually are): comment on Bowers and Davis (2012). (2012).
137 Baker, S.-A., Griffith, T. & Lepora, N. F. Degenerate boundaries for multiple-alternative decisions. *Nature communications* **13**, 5066 (2022).
138 Tajima, S., Drugowitsch, J., Patel, N. & Pouget, A. Optimal policy for multi-alternative decisions. *Nature neuroscience* **22**, 1503-1511 (2019).
139 Churchland, A. K., Kiani, R. & Shadlen, M. N. Decision-making with multiple alternatives. *Nature neuroscience* **11**, 693-702 (2008).
140 Kleiner, M., Brainard, D. & Pelli, D. What's new in Psychtoolbox-3? (2007).
141 Benjamini, Y. & Hochberg, Y. Controlling the false discovery rate: a practical and powerful approach to multiple testing. *Journal of the Royal statistical society: series B (Methodological)* **57**, 289-300 (1995).